LASER TRANSMISSION WELDING OF THERMOPLASTIC TUBES AND PLATES USING LASER REFRACTION

By

Rajaprakash Ramachandramoorthy

September 2011

Department of Mechanical Engineering
McGill University, Montreal, QC, Canada – H3A 2K6.

A thesis submitted to
McGill University
in partial fulfillment of the requirements of the degree of
Masters in Engineering

Abstract

Laser transmission welding is a method of joining plastics, which benefits from the infrared transparency in majority of thermoplastics. During the process, a laser beam passes through the laser transparent part and hits the laser absorbent part, which has been made absorbent using additives such as carbon black. The absorbed laser energy is then converted into heat and in turn welds the interface of the two parts by melting the polymer. In the current work, a new refraction technique of laser transmission welding is used to weld nylon plates to nylon tubes with carbon black. For the laser to refract, an angle was machined into the laser transparent nylon plates adjacent to the weld interface. Effect of different laser properties such as laser speed, number of laser rotations and laser power were studied on the quality of welding in terms of better finish and strength. The strength of these welds was assessed using a new tensile test fixture. Subsequently, the weld seam width was found from the tensile tested samples by analyzing the weld interface using vernier and transmission light microscopy. These tensile test results were then normalized using the weld seam area to obtain the tensile stress. The results showed the samples could withstand more tensile stress with an increase in laser power and rotation, excluding the samples which had decomposition due to excessive laser power. Also, the material property changes at the weld interface due to laser welding were characterized using a nanoindenter, for which small square samples were carved out of the weld interface and cold mounted. The results show that the modulus and hardness of nylon decreases right at the interface of the weld. In order to find the reason why there is a decline in the above mentioned mechanical properties, differential scanning calorimetry (DSC) testing was done to find possible changes in crystallinity, as decreasing modulus in semi-crystalline polymers is usually a result of decreasing crystallinity. The results confirmed that the crystallinity indeed decreased at the weld interface which would explain the decrease in mechanical properties.

Résumé

Le soudage par transmission laser est une méthode pour joindre les plastiques qui prend avantage du fait que la majorité des thermoplastiques sont transparent aux infrarouges. Durant le procédé, un faisceau laser passe à travers une région transparente pour aller en frapper une autre rendue absorbante au moyen d'additifs tel que le noir de carbone. L'énergie laser absorbée est ensuite convertie en chaleur. Ce dégagement de chaleur permet de souder l'interface entre les deux parties en fondant le polymère. Dans le présent travail, une nouvelle technique de soudage par transmission laser basée sur la réfraction a été utilisée pour souder des plaques de nylon à des tubes de nylon contenant du noir de carbone. Afin de réfracter le laser, une surface en angle a été usinée à même les plaques de nylon transparentes, près de l'interface de soudage. Les effets de différentes propriétés du laser telles que la vitesse, le nombre de rotations et la puissance ont été évalués en se basant sur la qualité du soudage en termes du fini et de la résistance aux contraintes. La résistance des soudures a été déterminée à l'aide d'un nouvel accessoire de test en traction. Ensuite, la largeur de la soudure a été mesurée sur les échantillons testés en traction à l'aide d'un pied à coulisse et de la microscopie par transmission de lumière. Pour obtenir la contrainte en traction, les résultats des tests en traction ont été normalisés en les divisant par la surface réelle de leur soudure. Les résultats démontrent qu'une augmentation de la puissance et de la rotation du laser, jusqu'au seuil de dégradation, permet aux échantillons de soutenir davantage de contraintes en traction. De plus, les changements dans les propriétés du matériel dus à la soudure ont été caractérisés à l'aide d'un nano-indenteur, pour lequel de petits échantillons carrés ont été extraits de l'interface de soudure et montés à froid. Les résultats démontrent que le module et la dureté du nylon diminuent à l'interface de soudure. Puisque la diminution du module dans les polymères semi-cristallins est habituellement associée à une diminution de cristallinité, la calorimétrie différentielle à balayage a été utilisée afin de déceler les possibles changements dans la cristallinité. Les résultats confirment en effet que la cristallinité diminue à l'interface de soudure, et expliquent donc, par le fait même, la diminution des propriétés mécaniques.

Acknowledgement

I would like to express my sincere gratitude to my thesis supervisor, Professor Pascal Hubert, for his invaluable guidance and encouragement during the course of this research work.

Special thank goes to Prof. Phil Bates from Royal Military College, Kingston, for his support and allowing me to use the laser equipments. I extend my thanks to Prof. Gene Zak from Queen's University for his comments and suggestions on various aspects of my research. I also would like to thank, Dr. Elizabeth Azhikannickal postdoc from Queen's University, Dr. Jorge Uribe-Calderon postdoc from McGill University for their intellectual discussions and support.

I further wish to thank my professors, colleagues and friends at the Composite materials and structures laboratory for providing a cordial learning environment. Specifically, I would also like to thank Ms. Erin Quinlan for her help in crystallinity studies. And a special thanks goes to Don and Bob from the electrical engineering department machine shop; without their advice and professional machining service none of this work would have been possible.

I further wish to thank my closest friends Ms. Mirunalini Thirugnanasambandam, Mr. Akhil Soman Thekkepurakkal and Mr. Mohammad Shahidzadeh Mahani, for their encouragement, motivation and constant moral support. I would also like to add my special thanks to my dearest sisters Ms. Inna Smirnova, Ms. Preethi Amarnath, Ms. Charmaine Cheung and Ms. Simran Dhaliwal, for being a constant source of encouragement throughout my studies.

Finally, I cannot thank enough my mother and father, Mrs. Porkodi and Dr. Ramachandramoorthy, and my grandparents, Mrs. Janaki Thiyagarajan (late), Mrs. Pachaikili Arumugasamy, Mr. Thiyagarajan (late) and Mr. Arumugasamy (late) for their never ending love and support throughout my life and career.

Table of Contents

List of Tables

List of Figures

Chapter 1 Introduction

Plastics are used extensively in a variety of applications including automotive components, electronics and medical devices. When a complex component cannot be injection molded in one piece, small pieces are injection molded and joined together using plastics joining techniques. One of the most commonly used techniques for joining plastics is welding. They can be broadly classified as thermal, friction and electromagnetic welding.

Laser transmission welding (LTW) is a type of electromagnetic welding, which uses laser radiation to join plastics, where one part is laser transparent and the other part is laser absorbent, which has been made so using additives such as carbon black. The laser radiation passes through the laser transparent part, hits the laser absorbent part where the laser energy is absorbed by the carbon black particles. These particles convert the laser energy into heat, which in turn melts the material to form the weld.

1.1 Project Objectives

Laser transmission welding has been researched for the past 15 years using simple geometries, to characterize the welding process. However, in order to apply this welding process in an industrial setting, it should be able to weld complex geometries. One such geometry which the industry is interested in welding is a curved joint of a tube to a plate. Previous research on welding the same geometry involves using static lasers and mirrors to reflect them, in order create the weld [1]. But it wasn't an industrially feasible idea as it required a metallic cylinder with a highly polished cone on top, to be inserted inside the tube to reflect the laser on to the weld interface.

One more possible solution to weld the same geometry is laser transmission welding through laser refraction. In this method the parts to be welded are stationary, but it is welded by a fast moving laser, which is programmable by the user. This method doesn't require a third material like the metallic cylinder in the previous research. The only different material requirement is the angle which needs to be machined in the laser transparent part in order to refract the laser on to the weld interface.

The objective of this research work primarily is to demonstrate that laser transmission welding using laser refraction is possible and it can be used to weld thermoplastic tubes and plates together. Then, the strength of the obtained welds will be tested using a tensile tester, to understand the quality of the weld. Also, nanoindentation will be employed to find out any possible material property changes at the local weld area. Finally, differential scanning calorimetry (DSC) will be used to characterize the crystallinity of the local weld area, in order to potentially explain the material property changes at the weld interface.

1.2 Thesis Organization

This thesis has been divided into six chapters. After the brief introduction to laser transmission welding in Chapter 1, Chapter 2 presents the information in literature related to this work. This includes a brief introduction to plastics, a background on various plastics joining methods, review of literature on laser transmission welding to join plates and tubes, a background of nylon-6 polymer and finally the reasons and motivations for this work.

Chapter 3 describes how the laser transmission welding was carried out using laser refraction, the methods and methodology involved, the various laser parameters varied and finally the visual rating of the welded samples.

Chapter 4 presents the methods by which the welded samples were tested for strength and local weld quality using tensile tester and nanoindenter respectively. The methods to find and confirm the weld seam width of the tensile tested samples are also mentioned.

Chapter 5 portrays the crystallinity studies of the welded material using differential scanning calorimetry (DSC), and how the crystallinity changes at the weld interface could explain the local weld quality.

Chapter 6 reviews the main conclusions of this research work and mentions possible areas for future work.

Chapter 2 Literature Review

This chapter introduces the background of plastics, different joining methods of thermoplastics and the chemistry of nylon-6 polymer used in this research. After weighing the pros and cons of different plastics and their joining methods and the gaps in literature, a detailed description of the motivations, reasons and organization of this research work is presented.

2.1 Plastics

Plastics are generally defined as materials which contain essentially one or more polymers of high molecular weight. They are broadly classified into two groups; thermoplastics and thermosets. Typically, thermoplastics are plastics which can be repeatedly softened by heating and hardened by cooling and can be shaped by flow into various articles in the softened state. They are usually filament molecules which are either amorphous or partially crystalline as shown in

Figure 1 [2].

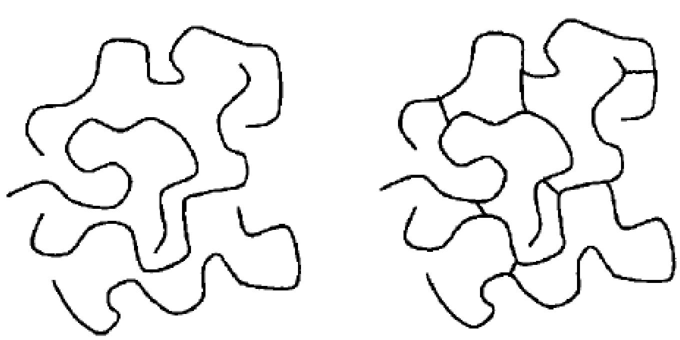

Figure 1: Thermoplastic and thermoset polymers [3]

Thermosets, on the other hand, are plastics which after being cured by heat or other methods, form a three-dimensional amorphous cross-linked molecular network that no longer softens or melts upon application of heat [2]. When excess heat is applied, thermoset materials will degrade.

2.2 Joining of Thermoplastics

Joining is one of the critical steps in manufacturing components from plastics and polymeric composites. The need for joints arises when part integration is not possible due to the complexity and/or cost and when disassembly is required. For example, due to limitation of injection molding, complex parts can be manufactured only by joining two or more injection molded parts [4]. Joining of thermoplastics can be classified as chemical, mechanical and welding or fusion bonding as seen in Figure 2.

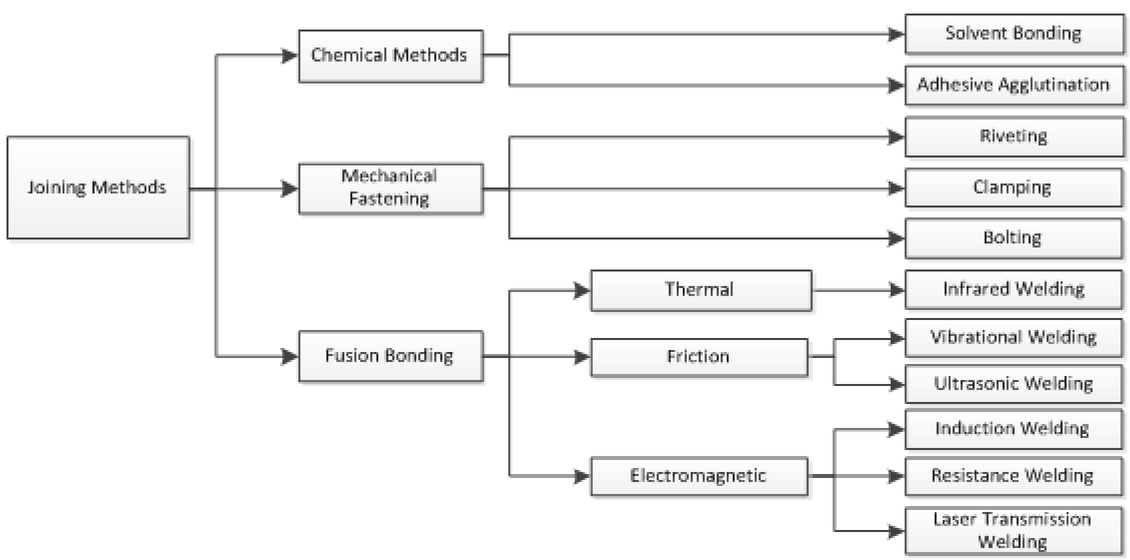

Figure 2: Joining methods of thermoplastics

In adhesive bonding which is one of the chemical methods of joining plastics, an adhesive is placed between the adherents such that the load is transmitted through the joint. Mechanical fastening usually involves the use of metallic or polymeric screws and snap fits. In fusion bonding methods, heat is applied to melt the polymer at the interface to cause chain entanglements and molecular diffusion across the interface, which in turn produces a solid welded joint upon cooling [4].

Since laser transmission welding falls under the fusion bonding category, only similar techniques such as infrared, vibrational, ultrasonic, induction and resistance welding will be discussed here.

2.2.1 Thermal welding

In thermal welding, an external heat source applies heat to the individual bonding surfaces to melt the matrix. Then the heat source is removed and the surfaces are brought together under pressure.

2.2.1.1 Infrared welding

Infrared welding comes under non-contact type thermal welding, where the surfaces to be bonded are heated using infrared radiation produced usually by quartz-halogen lamps, with filament temperatures in the range of 3000˚C [4]. The interfaces to be welded are heated through exposure to an intense narrow beam line of infrared heat without thermally damaging the adherends. Once the melt zone is created on both surfaces the parts are pressed together until the thermoplastic cools down [5] as shown in Figure 3.

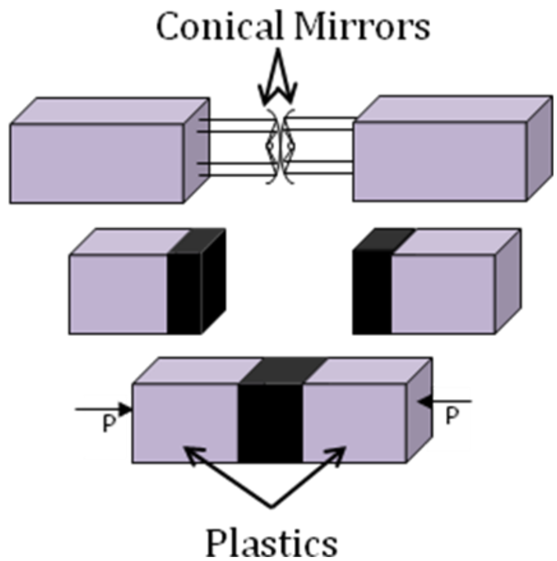

Figure 3: Infrared welding

2.2.2 Friction welding

Friction welding is a widely used technique for welding thermoplastics in industry, especially in the automotive sector. The welding process simply involves rubbing two thermoplastic interfaces together until the surfaces melt under mechanical friction and intermingle, and then they cool down to create the weld. This process is used when the complexity of the injection molded part does not facilitate manufacturing from a single piece [4].

2.2.2.1 Ultrasonic welding

Ultrasonic welding is a process that uses high frequency mechanical vibrations to weld thermoplastic parts. The parts to be welded are held under pressure and then subjected to high frequency oscillations to pass vibrations through the material. Heat in this method is generated by both surface friction and intermolecular friction. In order to concentrate the vibrational energy in a particular place, asperities need to be built into the material to act as energy directors. Once the asperities melt, this melted polymer flows under the application of pressure. This polymer flow wets the interface and entanglement of polymer chains takes place, which solidifies to create the weld [6], as shown in Figure 4.

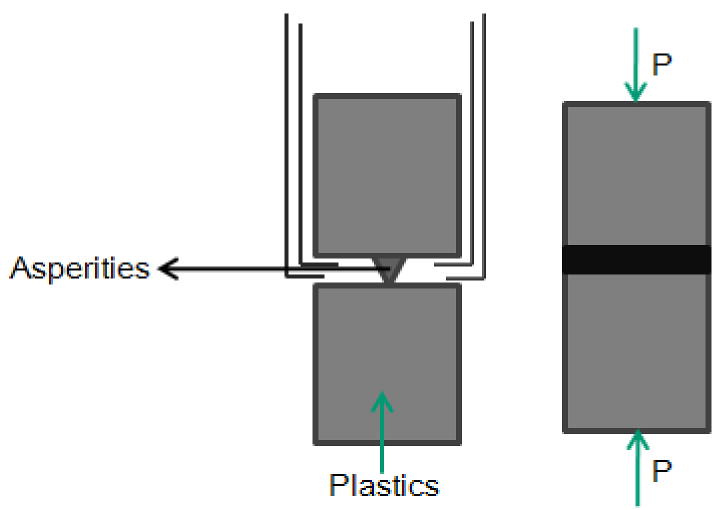

Figure 4: Ultrasonic welding

2.2.2.2 Vibration welding

Vibration welding is very similar to ultrasonic welding, but the frequency used in vibration welding is around 20 Hz which is a much lower than that is used in ultrasonic welding. In this welding, one part is fixed and the other is vibrated parallel to the interface until heat is generated by mechanical friction and shear stresses at the interface. This heat melts and mixes the thermoplastics together to form the weld [7], as shown in Figure 5.

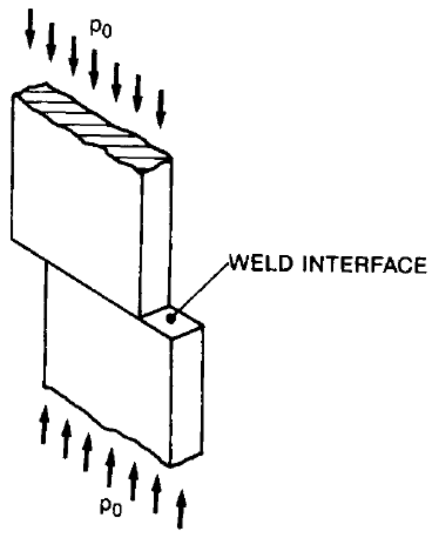

Figure 5: Vibration welding [8]

2.2.3 Electromagnetic welding

In electromagnetic welding of materials, firstly an opaque powder or an insert such as iron oxide, stainless steel, etc. is molded in the polymer matrix between the parts to be welded. Then, a high frequency magnetic field causes the magnetic materials at the interface to heat and start melting. This molten polymer diffuses under pressure to make the weld [7].

2.2.3.1 Induction welding

Induction welding process consists of heating a ferromagnetic implant in the interface of the two thermoplastics to be welded, using a high-frequency electromagnetic field from an induction coil. The electromagnetic field induces eddy currents within the implant, which in turn produces heat by resistance heating. This increasing temperature melts the surrounding polymer and the joint is kept under pressure until the polymer solidifies to result in a weld [9], as shown in Figure 6.

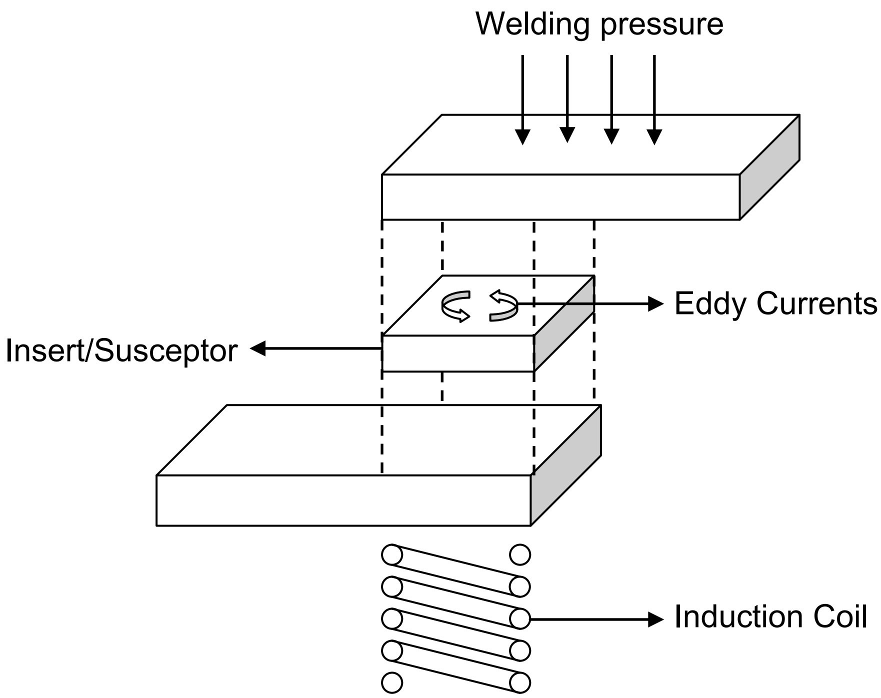

Figure 6: Induction welding

2.2.3.2 Resistance welding

Resistance welding, shown in Figure 7, is analogous to induction welding in many ways; the only difference being that here the electric current is directly passed through the heating element placed at the interface rather than using eddy currents generated by the induction coils. The heating element heats up due to Joule heating, which softens and melts the polymer at the interface. When there is enough melting of polymer, current is switched off and the joint is allowed to cool under adequate pressure until it solidifies to form the weld [10].

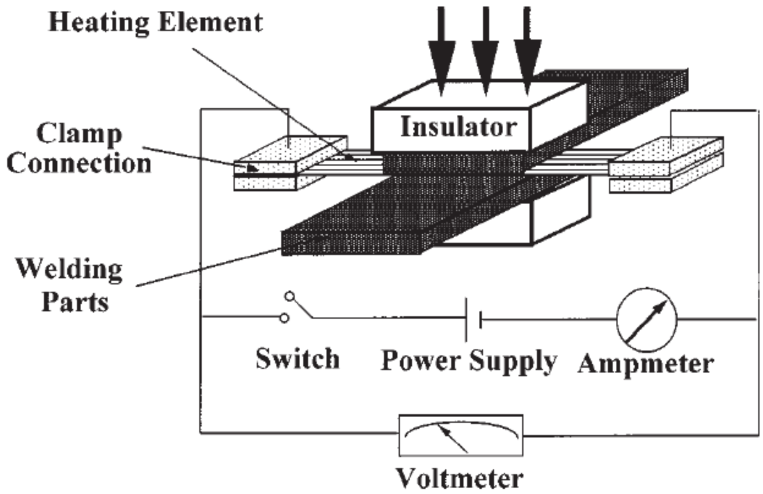

Figure 7: Schematic of resistance welding [11]

2.3 Laser Transmission Welding

In laser transmission welding, laser is used to form a weld between two thermoplastic parts - a laser transparent part and another part which has been rendered laser absorbent through compounding with appropriate additives such as carbon black, as shown in Figure 8.

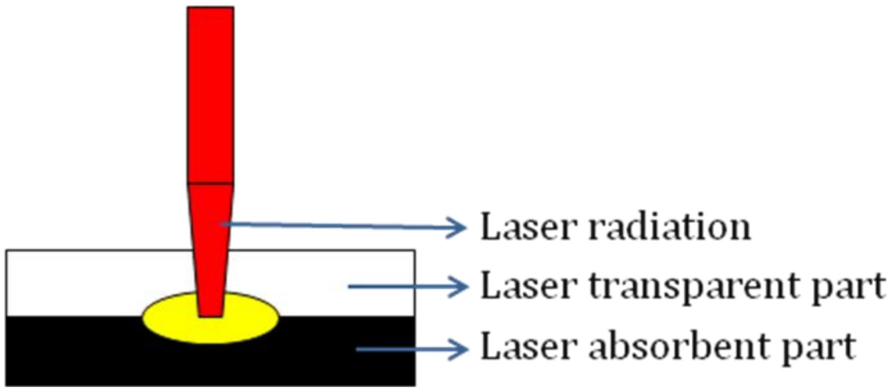

Figure 8: Laser transmission welding

Laser transmission welding for joining different kinds of synthetic resins using an Nd:YAG laser beam was patented by Nakamata in 1987, where styrene acrylonitrile polymer and the same polymer with 0.1 wt% carbon black were used as the laser transparent and laser absorbent parts respectively. This welding method was formulated based on the fact that polymers have a good transmittance of electromagnetic radiation from 400nm to 1600nm [12].

Since then, the technology of laser transmission welding has been developed to weld a variety of polymers including polycarbonates, acrylic, polyvinylchloride and polyamides using different types of lasers such as CO_2(~10600nm), Nd:YAG (~1600nm), and diode lasers (808-980nm). It is even possible to weld two components which are both black since the absorption and transparency behaviour of pigments in the visible range do not have to correspond to the optical behaviour in the laser wavelength. For example, one part can have carbon black added to it to absorb laser power, while the other part that is transparent to the laser beam includes a pigment which is transparent in the laser wavelength, but highly absorbent in the visible range to give it the black visible appeal [13]. In a similar way it is possible to weld two components which are transparent, using dyes which are transparent in the visible spectrum, but absorbing in the infrared spectrum [4]. Thus part color does not limit the use of laser transmission welding.

One of the important factors which affect laser welding is the energy lost due to reflection and absorption due to scattering from the laser transparent part. But thermoplastics like nylon-6 (described in detail in the next section) are not glasslike in surface. So the reflection from the surface is very minimal (~6%) when compared to the scattering inside the polymer matrix, which is mainly due to the crystalline structures such as spherulites [14-16]. Transmission after scattering in a polymer like nylon-6 is approximately 68% in its natural state without any additives or fillers [17]. When the polymer is mixed with laser absorbing additives such as carbon black, the optical penetration depth falls steeply [18], as shown in Figure 9.

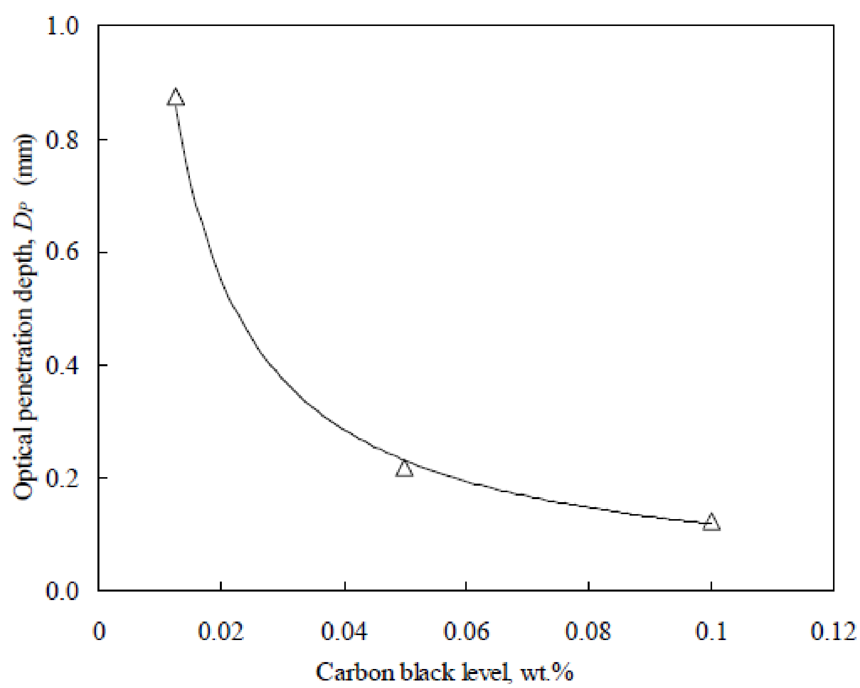

Figure 9: Optical penetration depth vs. Carbon black level [18]

In order to achieve a successful weld through laser transmission welding, a good understanding of the issues associated with the welding process is required. Polymer degradation and surface burning are the two key issues which affect the strength and the visual appeal of the weld respectively.

When the weld interface receives excess laser power than required, polymer degradation takes place. Surface burning of the laser transparent part, which also affects the visual appeal of the welded sample, is one of the signs that the sample receives excess power. Bubbles or vapour condensation at the bottom surface of the laser transparent part and the top surface of the laser absorbent part also indicate polymer degradation. The bubbles in the weld area are due to polymer degradation, which results in the formation of vapour that subsequently gets trapped in the weld interface. These bubbles are simply voids which reduce weld strength.

One of the ways to reduce polymer degradation is to have the two parts to be welded in very close contact. When the parts to be joined are in close contact, the local temperature at the weld interface will be lower due to the thermal conduction of heat on both sides of the weld. Even if gaps exist between the parts but the gaps are small enough to be closed by thermal expansion of materials, then polymer degradation will again be reduced.

It has also been proved that melt flow which is mainly caused by thermal expansion increases when there is thermal degradation. This occurs mainly when the samples are welded at a higher power. So in order to decrease flash - the overflow of material through the weld interface, polymer degradation should be prevented [19].

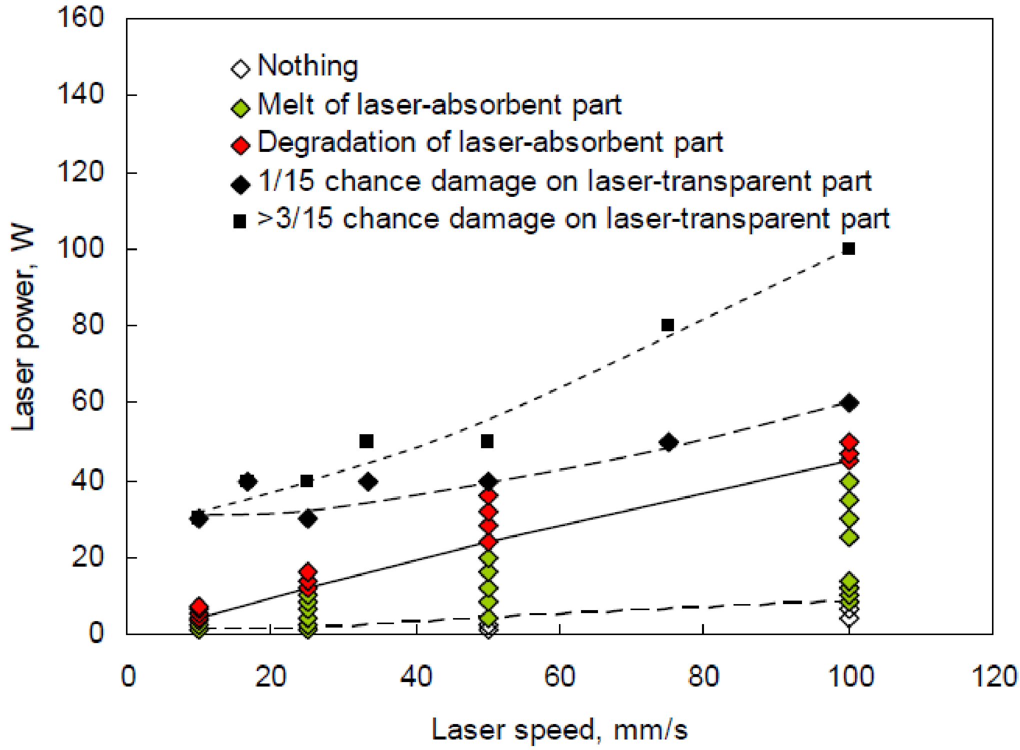

Figure 10: Surface burning and polymer degradation study [18]

From Figure 10, it can be seen that the surface burning of the laser transparent part increases with decreasing speed. This is due to the fact the surface burning is caused at the very thin top skin. Since the skin has low thermal inertia, it is more sensitive to heat loss by conduction and therefore to the speed of the welding process as well. But it can also be seen that polymer degradation is unaffected by the laser welding speed. The polymer degradation starts at a line energy, which is laser power divided by laser power of 0.5 J/mm for all laser speeds. So, if the line energy is kept between 0.1 J/mm, when the polymer starts to melt and 0.5J/mm, polymer degradation could be avoided and stronger welds could be achieved [18].

Laser transmission welding is currently used successfully to weld a variety of geometries including I-beams [16] and T-joints [20], as shown in Figure 11.

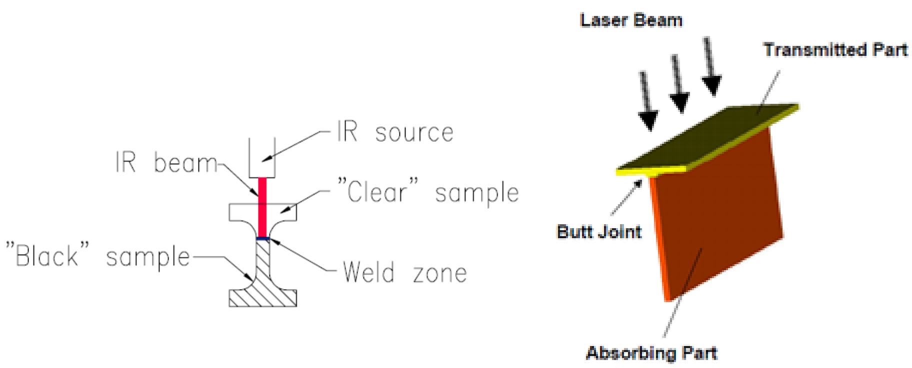

Figure 11: I-beam [16], T-type butt joints [20]

Tube and plate combination is another geometry that can be welded using LTW. In order to accomplish this, thermoplastic laser absorbent plates and laser transparent tubes are first set over a fixture which is rotated using a gear motor as shown in Figure 12. Then a metallic cylinder with a highly polished mirror-like cone on top is inserted into the thermoplastic tube. Subsequently, a stationary laser is shone from top. It gets reflected at the rotating polished conical surface, goes through the laser transparent tubes and reaches the laser absorbent plate, where the carbon black particles absorb the laser radiation. These particles convert them to heat, which in turn melts the thermoplastic materials. When this melt solidifies, the weld is formed as shown in Figure 13 [1].

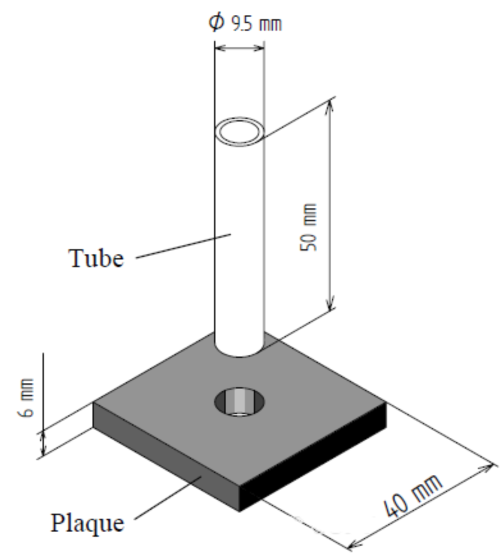

Figure 12: Dimensions of the thermoplastic tubes and plates [1]

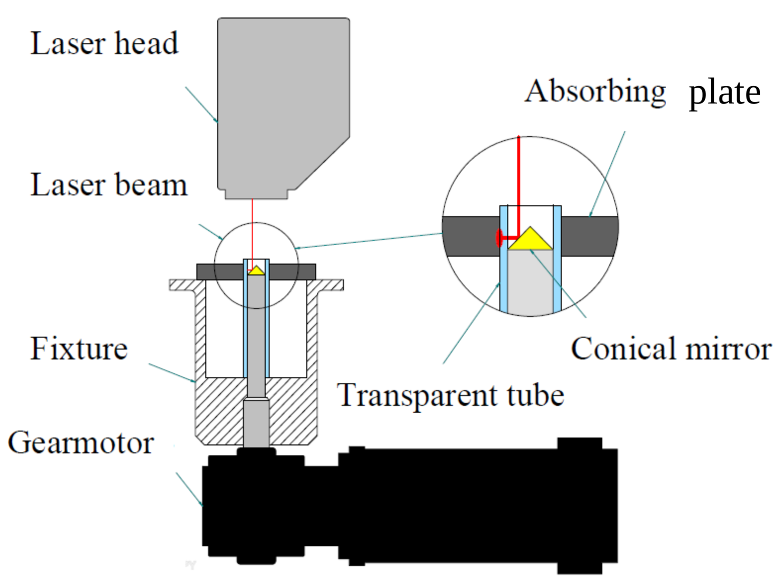

Figure 13: LTW of thermoplastic tubes and plates using laser *reflection* [1]

The strengths of weld obtained from this laser reflection weld averages 19.5 MPa and the speed of welding ranges from 100-250 RPM [1].

2.4 Nylon-6

Nylon was the first synthetic, semi-crystalline polymer with appropriate strength and temperature resistant properties which allowed it to be used as an engineering thermoplastic. This means that it is a thermoplastic which could match up to or even outperform metals in a few areas. Nylons in general are polyamides, which contain a repeating amide –CONH– group in the polymer chain [15]. Nylon-6, also known as polycaprolactum or polyamide 6, in particular is a low cost polymer with excellent physical and mechanical properties, whose chemical structure is shown in Figure 14.

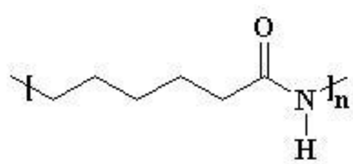

Figure 14: Nylon-6 chemical structure [21]

Semi-crystalline polymers such as Nylon-6 are usually considered in terms of two-phase models, since the polymer contains both crystalline and amorphous regions, as shown in Figure 15.

Figure 15: Semi-crystalline polymers [22]

2.4.1 Morphology of Nylon-6 crystals

The crystalline regions of nylon-6 can exist in two major forms, the monoclinic α–form and monoclinic or pseudo hexagonal γ–form [23-26], as shown in Figure 16. In the α–form, crystals have a monoclinic crystal structure and the hydrogen bonded sheets are composed of neighbouring chains traversing in opposite directions [27]. These crystals can be pinpointed using X-ray diffraction by identifying the two characteristic peaks at 2θ = 20 and 2θ = 23.7˚ [28].

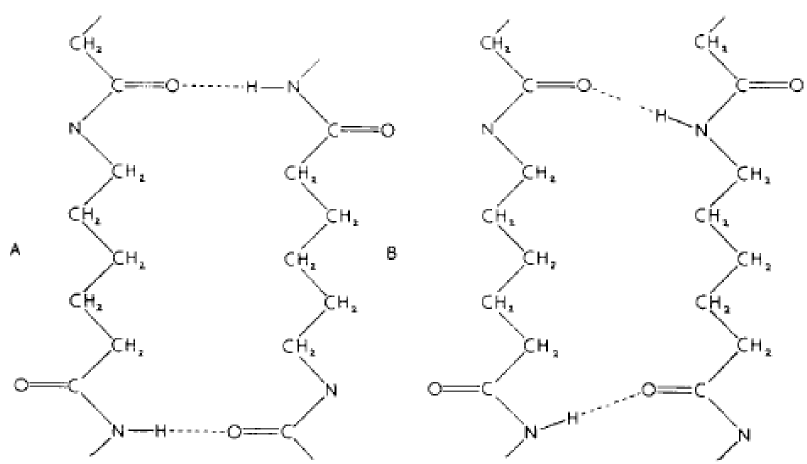

Figure 16: Nylon-6 α–form (A) and γ–form (B) [21]

In the γ–form the hydrogen bonds are between two parallel chains, which requires the polymer to twist away from the zig-zag plane, approximately 60˚ out of the sheets [27]. Simply put, the hydrogen bonding is intra-sheet in the α–form and inter-sheet in the γ–form. In X-ray diffraction these crystals are identified by the peak at 2θ = 21.4˚ [28].

In this work, the nylon plates were compression molded from virgin resin i.e. nylon-6 was made by pelletizing a strand of as-polymerized material. The samples with the required shape and geometry were then machined out of these plates. From literature, the crystallinity of compression molded nylon-6 plates were recorded so that those results could be compared to the crystallinity of the nylon-6 plates used in the present work.

Compression molding of virgin nylon-6 resin results in a mixture of α and γ-forms of nylon-6, as shown in the X-ray diffraction scan in Figure 17. But it is observed that the γ-form is found mostly in the outer skin of the molded part and the almost pure α-form of nylon-6 is present in the central or core part of the molded plate [29]. This phenomenon can be attributed to the fact that rapid cooling favours γ-form and slow cooling favours the α-form [27]. Also, since the outer skin cools faster than the central core of the compression molded plates, it favours γ-form growth near the skin.

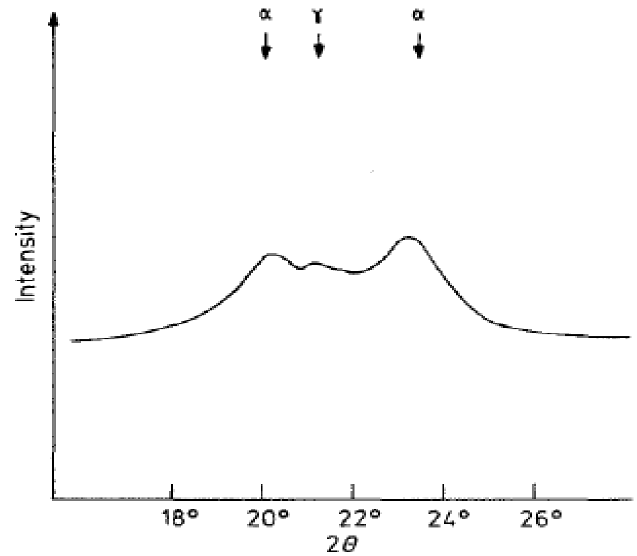

Figure 17: X-ray diffraction scan of a compression molded nylon-6 [28]

2.4.2 Crystallinity vs. mechanical properties

For semi-crystalline polymers such as nylon-6, the morphology of crystals and percentage of crystallinity correlate directly with engineering parameters and physical properties. There are studies which prove that the different chemical structures of α and γ-forms of nylon-6 provide different physical and mechanical properties [30, 31]. The percentage difference in hardness and elastic modulus between α and γ-forms of nylon-6 has been found as 53 and 50% respectively. The reason for this difference has been attributed to the difference in packing density of the polymer chains and the number and strength of the hydrogen bonds. The crystals in the γ-form are also known to revert gradually to the α-form when the crystallization temperature is increased [30]. Also, for bulk semi-crystalline polymers such as nylon-6, it is a known fact that modulus, hardness and density increases, while toughness decreases with an increase in the percentage of crystallinity [15].

2.5 Reasons, motivation and organization of this work

2.5.1 Reason for using Nylon-6

The reason for choosing a thermoplastic material in this research is that, thermoplastic polymers, which are made of monomers attached to each other to form long chains, diffuse across the interface and form a bond through entanglement of chains when welded. Since the thermal conductivity of thermoplastics is low, the cooling rate after irradiation is sufficiently low for the formation of strong bonds. This gives thermoplastics a clear edge over other metals where heat is easily transported away from the weld area [32].

The reason for choosing nylon-6 was mainly because the industry is extremely interested in this material due to its lower weight, lower cost and better functionality than alternative competing materials such as magnesium alloys and other plastics. This is confirmed by the statistic that polyamide is the second largest plastic consumed by the industry at 1,950,000 tonnes per year around the world and the growth of consumption is approximately 8.5% per annum [33].

The automotive sector is the largest market sector for polyamide accounting for 34% [34]. Nylon is used for under-the-bonnet, electrical, lighting, exterior and interior applications in the automotive industry. Under-the-bonnet applications include air-intake manifold, intercooler, cylinder head over and engine parts. This research which focuses on the welding of tubes and plates using laser transmission welding is vital for the intercooler and other interior applications. But one of the minor disadvantages of using plastics in cars is the difficulty in recycling. Currently, more than 75% by weight of an average car is recycled, but most of the material recycled is sheet metal, plain steel, cast iron and aluminium [34]. The plastic parts on the other hand are often small and difficult to dismantle. Hence only few large parts such as bumpers and instrument panels which can be easily identified and dismantled are suitable for mechanical recycling. But since the amount of plastics in vehicles are growing further due to the need to reduce CO_2 emissions using lighter cars, the pressure also grows for more plastic recycling [35].

2.5.2 Advantages of laser transmission welding

The advantages of using laser transmission welding over other plastics joining methods are tabulated in Table 1. It can be clearly seen that, problems such as long cycle times, high manufacturing cost, mechanical impact, surface damage, and flash/melt overflow can be avoided by using laser transmission welding to weld plastics.

2.5.3 Laser welding using refraction

Laser transmission welding of tubes and plates by Anton et al., used a mirror-like polished cone to reflect the laser to carry out the welding. Even though the method was successful in creating a weld, the feasibility of the method to be used in an industrial setting is not very high. This was primarily due to the fact that, this method uses a stationary laser and the fixture had to rotate to make the weld between the tube and plate. This implied that the speed of the process is limited to the speed of the gear motor which rotates the fixture. Also, a metallic cylinder with a highly polished surface needed to be inserted inside the tube to successfully carry out the welding. Finally, the strength of the welds obtained were just 1/4th the strength of the natural nylon-6 material.

But this newly proposed technique of laser transmission welding using laser refraction rectifies many of the shortcomings of this previous method of welding tubes and plates together. Firstly, the laser refraction welding method uses quasi-simultaneous laser instead of a single diode laser. Quasi-simultaneous laser shown in Figure 18 also uses a single laser beam but the path of this laser is controlled by two mirror systems, which are in turn controlled by user programmable galvanometers.

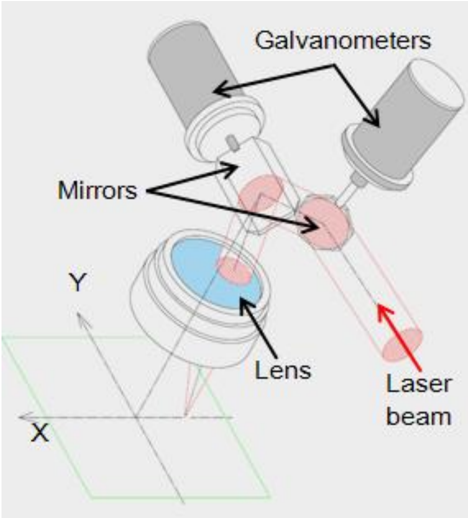

Figure 18: Quasi-simultaneous welder [1]

In this method, the sample which needs to be welded remains stationary and the laser moves to make the weld at a speed of 5.21 m/s. Thus the time taken for welding using the laser refraction method is 5-8 sec. Also, this method uses an exactly opposite setup of tubes and plates as compared to that used in the laser reflection method, as this method uses laser absorbent tubes and laser transparent plates. The laser transparent plates have angles machined on them in order to refract the laser onto the weld interface as shown in Figure 19.

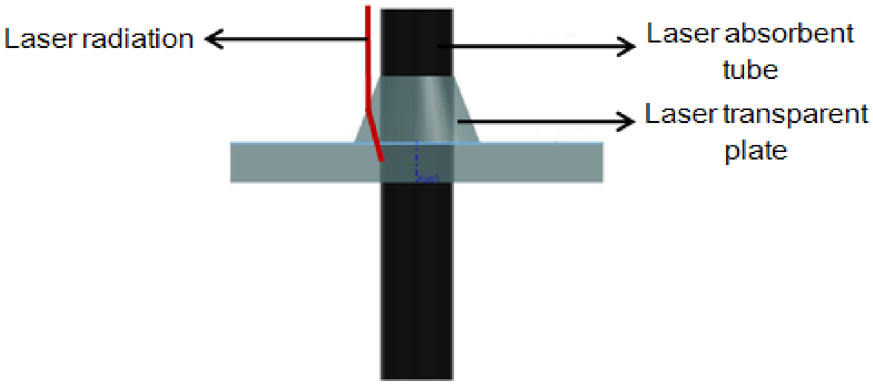

Figure 19: Setup used for laser refraction welding

The only material requirement for the industry to implement this welding process, besides the carbon black particles in the laser absorbent tubes, is the angle which has to be machined on the laser transparent plate.

2.5.4 Crystallinity of the weld

There are various methods for welding semi-crystalline polymers (e.g.: nylon-6). The crystallinity of compression molding and injection molding of such polymers have been analysed in detail in literature. But the crystallinity of such polymers at the weld interfaces after they have been joined together has not been looked into, which is a major gap in literature. Since the crystallinity directly affect the mechanical properties of the material, understanding how the crystallinity changes with welding will give a better insight into how the material will perform after the welding process.

Table 1: Comparison of plastics joining methods [3, 5, 7, 9, 36, 37]

	Laser transmission welding (LTW)	Mechanical fastening/Adhesives	Infrared welding	Ultrasonic/Vibration welding	Resistance/Induction welding
Mechanical impact	None	Minimal	None	Huge	None
Surface damage	None	Huge	Minimal	Minimal	Minimal
Visual rating of weld	Invisible to naked eye	Fair	Bad	Bad	Bad
Tool wear and tear	None	Minor	Minor	Major	Minor
Melt overflow	None/Minor	Minor	Major	Major	Major
Cycle time	5-8 sec	12-24 hours	3-5 mins	20-25 sec	30 sec-5mins
Weld quality (MPa) Strength of natural nylon-6 = 80 MPa	40	10-30	30	35	40
Investment costs	Big	Small	Intermediate	Intermediate	Intermediate
Part Size	Small and large	Small and large	Small	Small	Small
Manufacturing cost / sample (Comparative as the cost depends on the size and complexity of sample)	$50	$70	$50	$60	$60
External pressure (MPa)	None	0.1-1	0.1-1	1-4	0.1-1.4

Chapter 3 Laser Refraction Welding

This chapter explains the materials, equipments and methods used to carry out laser refraction welding. Also, the results of visually rating the welds between nylon tubes and plates are discussed.

3.1 Experimental Methodology

The two types of nylon parts required to do laser refraction welding are the laser absorbent tubes and laser transparent plates with angles machined in them to refract the laser radiation. The laser transparent 12.7mm (½”) thick, 304.8 mm by 304.8mm (12” by 12”) nylon-6 sheets were purchased from McMaster-Carr Supply Company (product code 85055K11). These sheets were then cut into small 5cm by 5cm, 12.7mm (½”) thick squares, and the angles ranging from 15 to 60 degrees were machined on them, along with a hole of 9mm diameter in the centre. The end result of this machining is shown below in Figure 20.

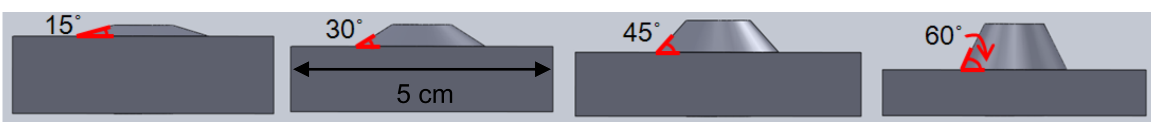

Figure 20: Laser transparent nylon-6 plates with angles for laser refraction

The laser absorbent tubes should ideally be manufactured from granules of nylon-6 with 0.2 wt% carbon black using an extruder with a conformer attached to it. But since a conformer wasn’t available for the project, tubes could not be manufactured. Instead it was decided to make laser absorbent rods (shown in Figure 18) by machining compression molded nylon-6 with 0.2 wt% carbon black plates. Hence, the nylon-6 with 0.2 wt% carbon black granules were first compression molded at 250 ˚C and cooled at a controlled rate of 15 ˚C/min. One of the issues encountered during the process of compression molding was the presence of air bubbles inside samples from the moisture absorbed by nylon-6, which could potentially prove detrimental to strength of the weld. In order to avoid the air bubbles in the sample, during the melting stage, the mould was opened for a few minutes to allow the air inside the sample to escape. Then using CNC machining these compression molded plates were first machined into rectangular bars as shown in Figure 21. These rectangular bars were then machined again using CNC into rods with a diameter of 9mm, which is also depicted in Figure 21.

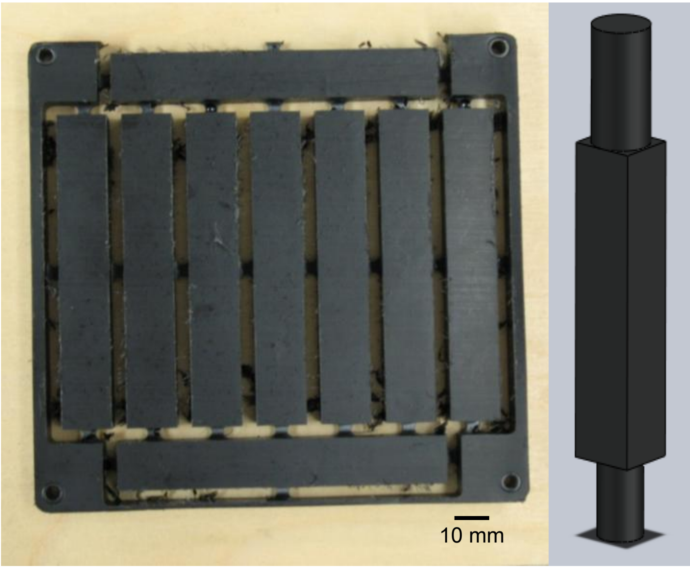

Figure 21: Sample preparation of laser absorbent rods

The summary of material properties and preparation of these two nylon parts are given in Table 2.

Table 2: Material properties and sample preparation

	Laser transparent plates	Laser absorbent rods
Material	Nylon-6 plates (Commercially bought 12” x 12” x ½” plates)	Nylon-6 with 0.2 wt% carbon black granules
Manufacturer	McMaster Carr (Product code: 85055K11)	DSM Engineering Plastics (Product code: Akulon F223-D)
Melting Point (˚C)	221	220
Method of sample preparation	Machining into smaller 5cm x 5cm plates -> Machining 15-60 degree angles on these plates -> Drilling holes at the centre of diameter 9mm	Compression molding into plates -> Machining plates into rectangular bars -> Machining bars into rods of diameter 9mm

These two parts of the sample were put together, ensuring tight contact between them by manufacturing them with the same diameter, excepting the machine tolerances. The tolerance or the interfacial gap between the tube and plate was measured using reflection microscopy, as shown in Figure 22. This was found to vary from 20 to 25 microns, which was well within the boundary of the appropriate gap required to create a strong weld through laser transmission welding [38].

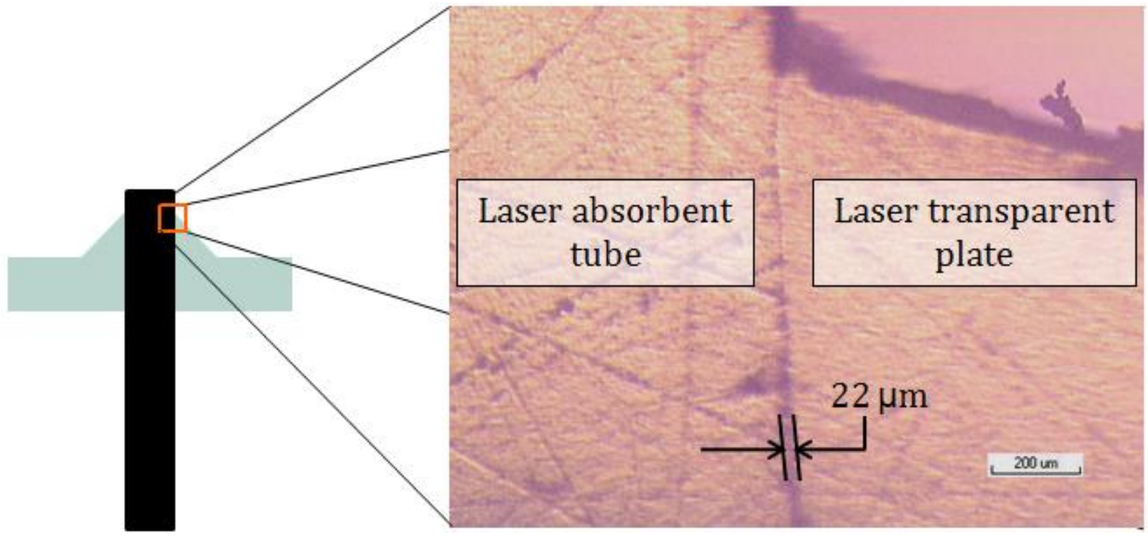

Figure 22: Interfacial gap measurement using reflection microscopy

3.1.1 Quasi-simultaneous laser welding

The quasi-simultaneous welder used in this research is a fiber laser welder from Biolematik (Product Code: K3621). The maximum power output of the laser is 250 W and the maximum scan area is 540 mm by 540 mm. This laser can be manipulated using scanning mirrors at a high processing speed around 6 m/s, and due to this high processing speed, the entire joint surface can be simultaneously heated and plastified with the single laser beam.

After the samples were put together as shown in Figure 22, the quasi-simultaneous laser was switched on. The laser beam was programmed in such a way that it was focused at 2mm from the top of the angled part for all the welded samples, as shown in Figure 23. The laser travels through the laser transparent plate after getting refracted inside due to the machined angle, hits the laser absorbent tube, and creates the weld at the interface.

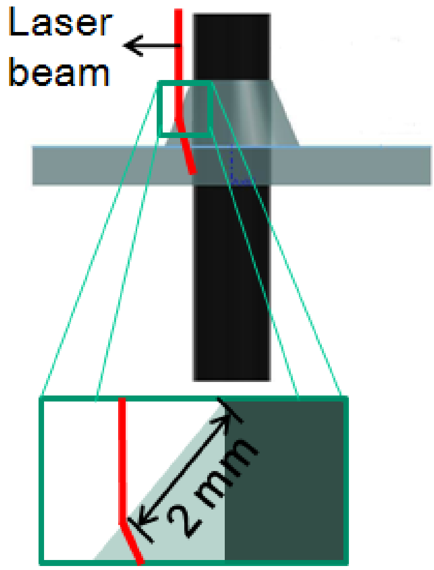

Figure 23: Laser refraction welding – laser incidence point

The test matrix used in the project involved changing the various laser parameters such as the laser speed, number of laser passes, laser power, and the refraction angle of the laser transparent plate. The variables which were used in this research are summarized in Table 3. The testing methodology used for welding every batch of samples with the same refraction angle was: fix the number of laser passes at 800 or 1000 and use the highest possible laser speed, then vary the laser power from 60 to 125.

Table 3: Laser parameters used in this study

Refraction angle	15˚, 30˚, 45˚, 60˚
Laser speed	Maximum speed of laser = 5.2 m/s
Number of laser passes	800 and 1000 rotations
Laser power (W)	60, 75, 100, 125

3.1.1.1 Motivation for using various angles

In this work, both small and large angles were used in the laser transparent plate in order to refract the laser radiation. The main reason and motivation for using different angles was industrial applicability. For example, the industry can sand down small angles such as 15˚ and can use a temporary attachment with larger angles such as 45˚ and 60˚, which is put on top of the plate to refract the laser as shown in Figure 24. Since the point of incidence of the laser can be controlled as shown in the previous section in Figure 23, it can be made sure that the laser refracts and meets the laser absorbent tube below the angled section next to the plate. Once the welding process is completed, the angled part can be removed. The calculations used to find the point where the laser refracts and meets the laser absorbent part is explained in detail in the next section 3.1.1.2. Thus the resulting welded part has more visual appeal which is also vital to the industry.

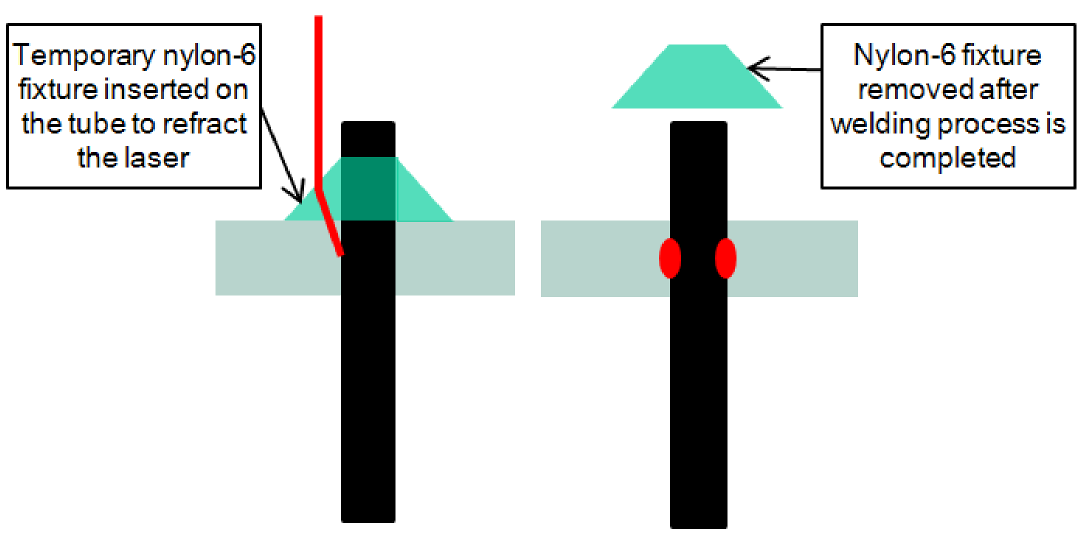

Figure 24: Temporary fixture with large angles to refract laser

3.1.1.2 Laser refraction

Laser, which is simply amplified light, still obeys Snell's law (Equation 1) with regards to refraction. Thus, using the calculations shown below, by controlling the incidence point of the laser, the point where the laser gets refracted and meets the laser absorbent tube can be found.

For example, if the laser is focused at 2mm from the top of the 45° (θ_i) plate as shown in Figure 25, using Snell's law (Equation 1), the laser's refracted angle, θ_r, can be calculated.

$$\sin(\theta_i) / \sin(\theta_r) = \text{Refractive index} \qquad (1)$$

Subsequently, both the distance travelled by the laser inside the laser transparent plate, D_{laser}, and the distance of the point from the top of the angled part to the point where the laser meets the laser absorbent tube, D_{tube}, can then be calculated using the laser's refracted angle and the dimensions of the angled part using basic trigonometry. For this particular example, the laser hits the laser absorbent tube at 2.9 mm from the top of the plate or at 5.9 mm from the top of the angled part. Thus, if the angled part had been a temporary fixture over the plate after the welding process was completed, the angled part can be removed and reused repeatedly. But it should be noted that, since the different angles were machined on the laser transparent plates in this research work, the temporary fixture concept was not tested.

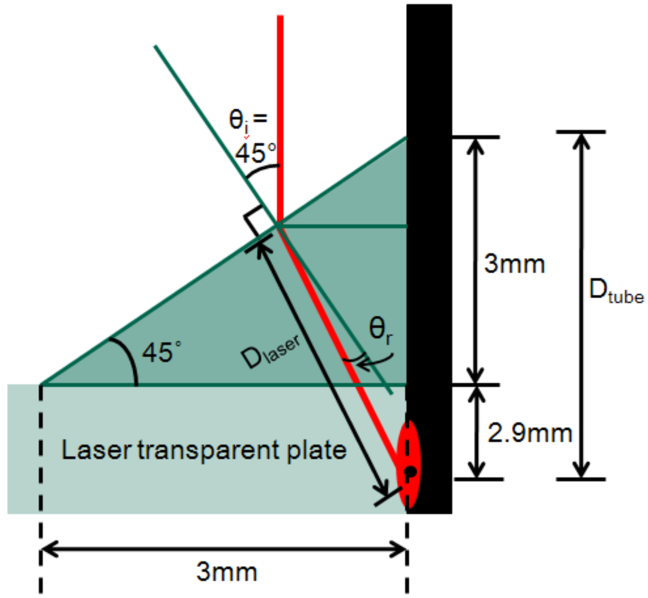

Figure 25: Calculation of the point where the laser hits the laser absorbent tube

3.1.1.3 Laser power study

When the laser beam hits the angled laser transparent plate, some of the laser power is lost due to the laser reflection from the surface. Higher the angle of the laser transparent plate, more the reflection off the surface. Also, when the laser gets refracted and travels inside the laser transparent plate, the laser powered gets scattered, as shown in Figure 26. This is due to the fact that nylon-6 is a semi-crystalline material. And as mentioned in the literature review, semi-crystalline materials have crystalline structures such as spherulites and lamellae which scatter laser radiation. So, the longer the laser radiation travels in the transparent plate more the scattering of the beam. And since the incidence point was kept consistent at 2mm from the top of the angled part, for higher angles the laser had to travel longer distances inside the laser transparent part and thus resulting in more laser scattering.

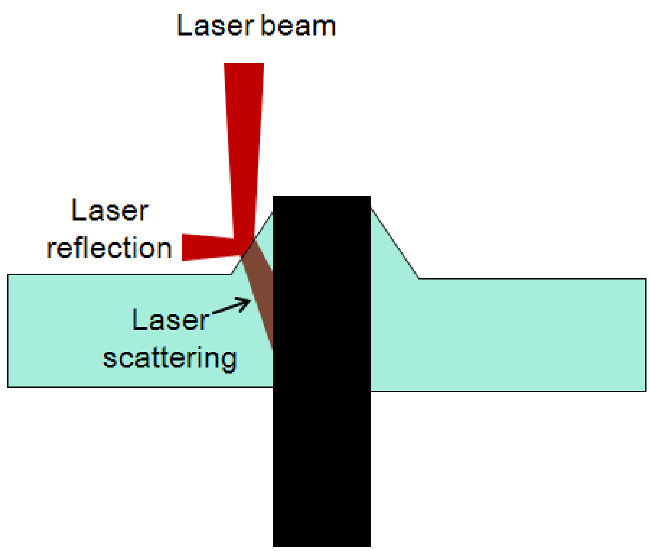

Figure 26: Laser reflection and scattering

Once the laser beam hits the laser absorbent rod, the carbon black particles absorb the laser power converting them to heat. So, for every rotation of the laser around the circumference of the rod, the temperature at every point in the weld interface increases and also decreases a little before the laser hits the same point again during the next rotation [39], as shown in Figure 27. When the temperature of the weld interface reaches 220˚ C, both the materials start to melt, and then intermingle to form the weld. But when there is too much power or too many rotations of the laser and if the temperature of the interface goes beyond the melting point of the material to around 350˚ C [40], the material starts to degrade.

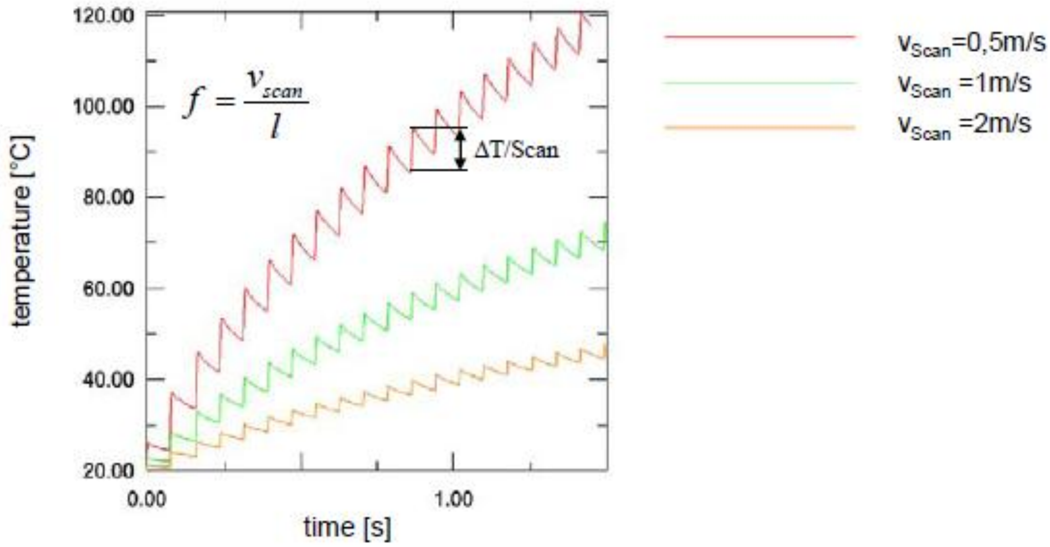

Figure 27: Temperature increase with laser rotations [39]

3.2 Results and Discussion

Using the test matrix mentioned in section 3.1.1, the laser refraction welding was successfully carried out and an example of the result is shown in Figure 28. Thus, the concept of laser transmission welding of tubes and plates using laser refraction was proved. *The complete list of samples welded for every laser* parameter is listed in Appendix A.

Figure 28: Example of a welded sample

Once the welding was completed, the samples were rated according to their visual appeal as weak, strong, minor and major flash welds, as listed in Table 4. Weak weld were the ones which were literally shaking in hand after the welding process was completed and these welds failed with very minimal resistance in hand. The reason for the weak weld could be either because the materials didn't reach the melting temperatures or the melting happened at few discrete spots in the weld interface. Strong welds on the other hand were the welds which couldn't be broken by hand and these samples had no overflow of the melted material from the interface. Thus they had a better visual appeal. There were also certain welds, where the melted material had over flown from the weld interface as shown in Figure 29. They were classified as minor and major flash welds.

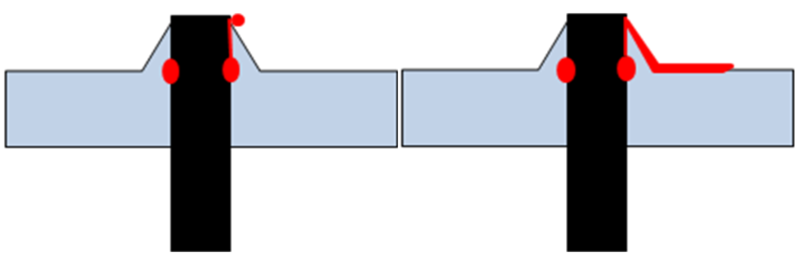

Figure 29: Minor and major flash welds

Minor flash welds are the ones where only a tiny amount of plastic overflowed out of the interface, while the major flash welds had a huge amount of over flow of the melted material. Since the visual appeal of the welded samples is also vital to the industry, strong and minor flash welds (e.g., when using 75W and 100W) are preferred.

Table 4: Visual rating of the welded samples

Angle \ Power	60W	75W	100W	125W
15°	No weld/ Weak weld	Strong weld	Strong weld/ Minor Flash	Minor Flash
30°	No weld/ Weak weld	Strong weld	Strong weld/ Minor Flash	Minor Flash
45°	No weld/ Weak weld	Weak weld	Strong weld/ Minor flash	Major flash
60°	No weld/ Weak weld	Weak weld	Strong weld/ Minor flash	Major flash

Chapter 4 Mechanical Characterization of Weld

This chapter explains how the successfully welded tubes and plates were tested for strength and local weld quality. Results of these tests are also described, along with the perceived reasons for this behaviour.

4.1 Experimental Methodology

After the welding process was completed, the welds were characterized for strength using tensile testing. Also, nanoindentation was used to ascertain any material property changes at the weld interface.

4.1.1 Tensile testing

The welds were tensile tested using MTS insight 5 machine with a 5 kN load cell, and the rate of testing was kept constant for all samples at 5mm/min. A tensile testing fixture was machined out of steel to test the weld, as shown in Figure 30.

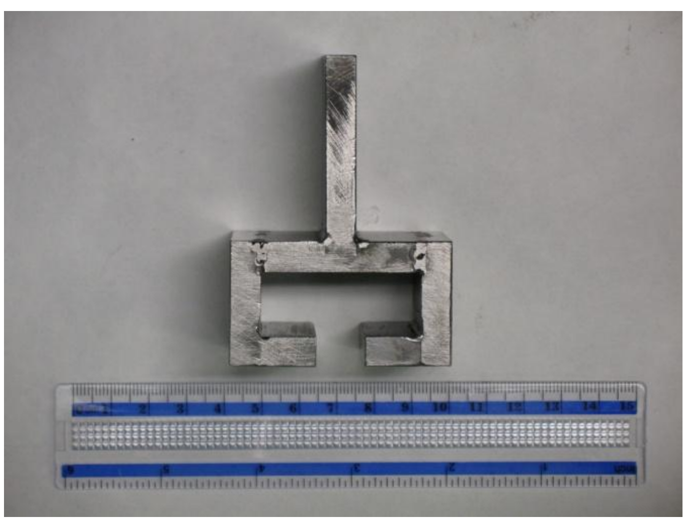

Figure 30: Tensile testing fixture

The welded sample was inserted in the fixture (Figure 30) and the sample was pulled apart using the grippers in the MTS machine, until the welds failed, as shown in Figure 31.

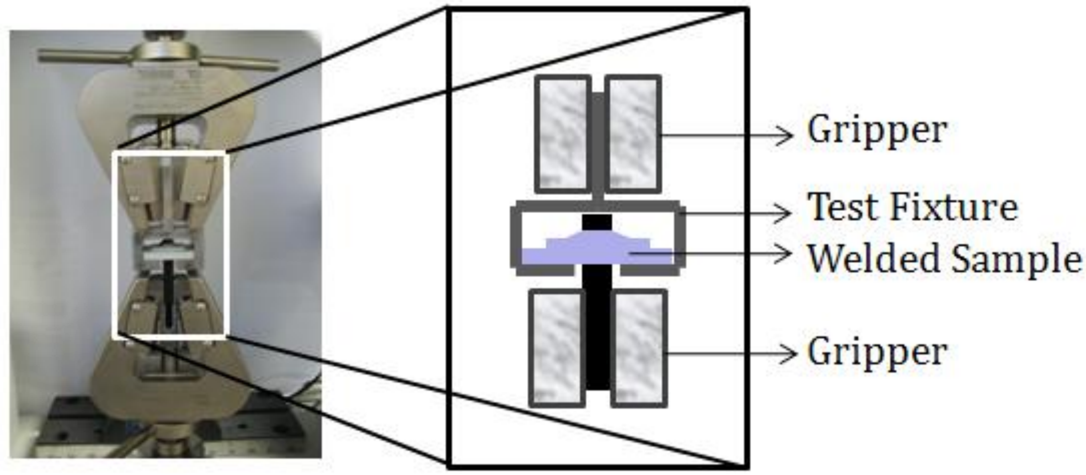

Figure 31: Tensile testing the welded sample

4.1.2 Nanoindentation

In order to find the material property changes at the local weld area, nanoindentation was used. To expose the weld area for nanoindentation, the samples were cut along the blue lines, as shown in Figure 32.

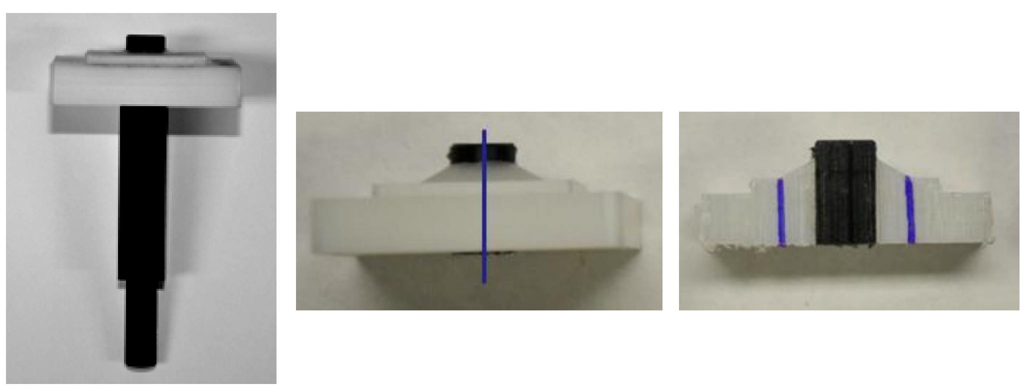

Figure 32: Nanoindentation sample preparation

Subsequently, the cut samples were cold mounted using epoxy resin and hardener, as shown in Figure 33. This was done to facilitate fine polishing of the samples, as the samples needed to be smooth for successfully carrying out nanoindentation.

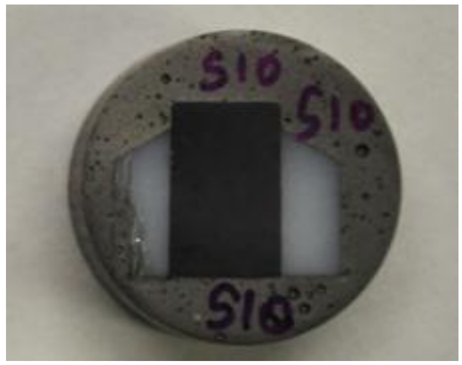

Figure 33: Cold-mounted nanoindentation sample

Hystrion Triboindenter using a Berkovich tip was programmed to perform nanoindents in straight lines, as shown in Figure 34. The indents start at the laser absorbent nylon rod, pass over the weld zone and finally end at the laser transparent nylon plate, with a gap of at least 50 microns between each other to avoid interactions. The load used for the indents was 10 mN. This load was held for 60 sec before unloading to avoid creep that could significantly affect the unloading behaviour [30]. The modulus of the material was then calculated using the maximum load, maximum displacement and the slope of the upper portion of the unloading curve [41].

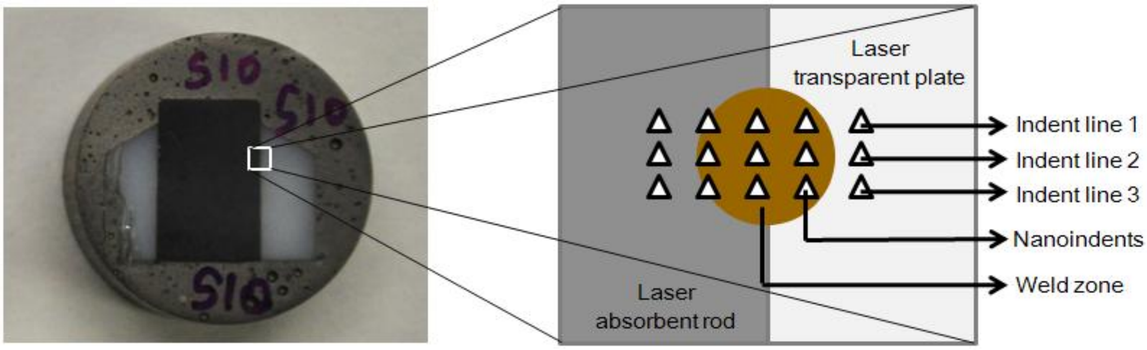

Figure 34: Nanoindentation profile

4.2 Results and Discussion

4.2.1 Weld seam width analysis

Tensile testing resulted in the failure of the weld, resulting in the separation of the welded samples into rods and plates as shown in Figure 35. One of the important parameters; the weld seam width, which is the width of the laser affected zone at the weld interface, was studied from the separated laser absorbent rods, as shown in Figure 35.

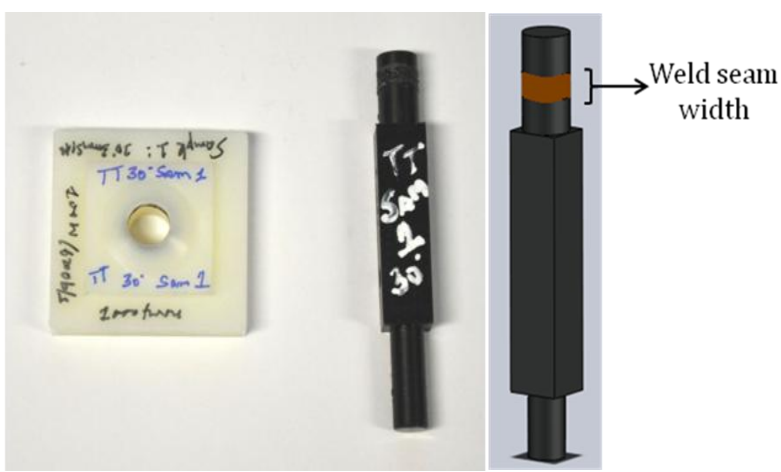

Figure 35: Welded sample after tensile testing and weld seam width

The measurement was made using vernier calliper and was confirmed by transmission light microscopy, which in turn measured the width of the heat affected zone as elucidated in Figure 36.

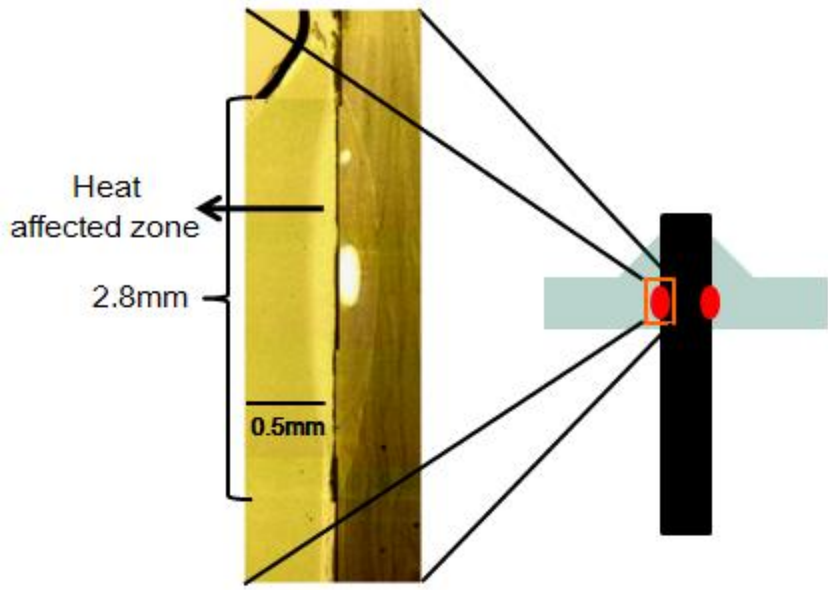

Figure 36: Weld seam width measurement using transmission light microscopy

The weld seam width results were in correlation with the visual rating of the welded samples, as tabulated in Table 5. So, in order to get the preferred strong and major flash free welds, the weld seam width should be between 3 and 4 mm.

Table 5: Comparison of weld seam width with visual rating

	Weak Weld	Strong Weld / Minor Flash	Major flash
Weld Seam Width	1.5 – 2.2 mm	3 - 4 mm	> 4.5 mm

4.2.2 Weld Strength

During tensile testing of the welded samples, load and extension data was collected from the tensile tester. A typical load-extension curve of a 30° sample welded at 100 W with 800 laser rotations is plotted in Figure 37. As it can be inferred from the graph, the load increased till the failure of the weld, beyond which it dropped immediately.

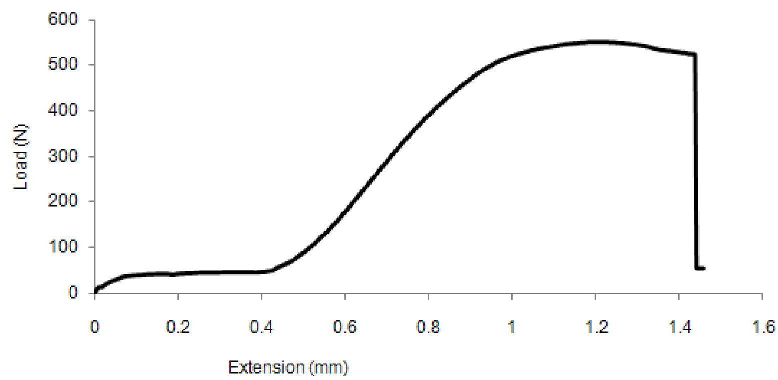

Figure 37: Typical load-extension curve of a weld using laser refraction

From the load-extension data, the failure load for every tensile tested sample was collected and was plotted against the various laser parameters (number of laser rotations and laser power) used in the test matrix. In Figure 38 the graph for the 60˚ samples is plotted. From the figure, it is evident that the when the samples were welded with 1000 laser rotations, the welds were stronger compared to the samples welded with 800 laser rotations. Furthermore, it can be seen that there is a decrease in the failure load for the samples welded at 100 W with 800 laser rotations, which cannot be explained using the laser power study in section 3.1.1.3. These aberrations in the failure load were also found in samples with other refraction angles (15, 30 and 45 degrees). In order to reduce these aberrations, the failure load was normalized with the weld seam area, (which is the weld seam width multiplied by the circumference of the rod) to obtain the weld shear strength. When the weld shear strength was plotted against the power, as shown in Figure 39, it can be seen that the aberrations were not present.

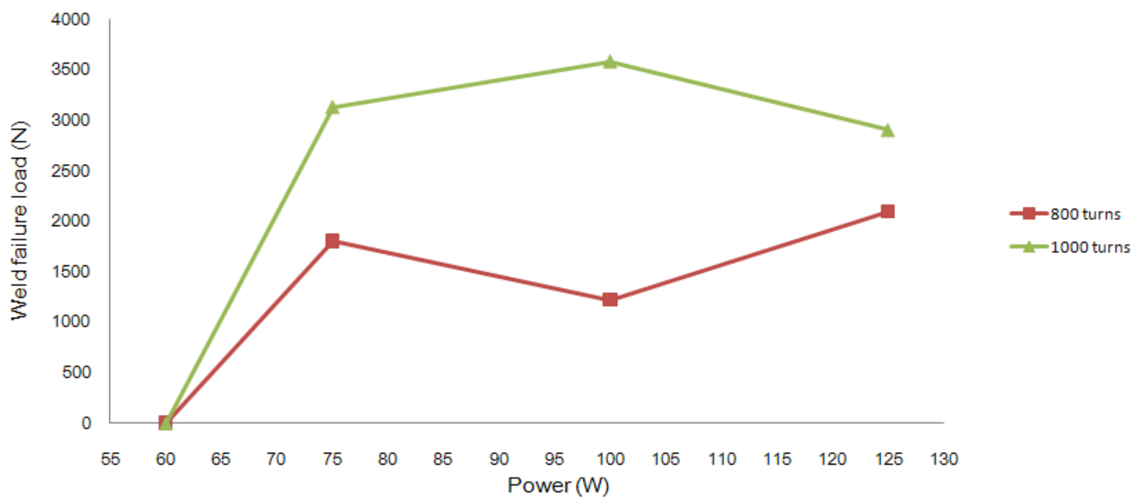

Figure 38: Weld failure load vs. power for 60 degree samples

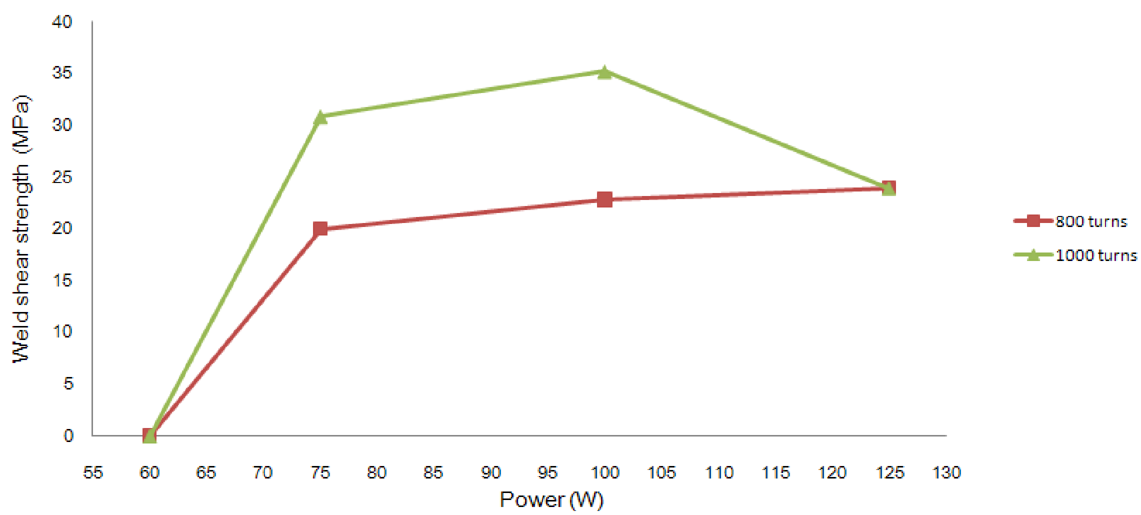

Figure 39: Weld shear strength vs. power for 60 degree samples

As seen from Figure 40, when the weld shear strength of samples with different refraction angles are plotted against the laser power they were welded with, the shear strength increases with increasing power. But it should also be noted that for the 15 degree samples the slope of increase in shear strength with power, is higher compared to the samples with higher refraction angles. Also, it can be seen that for 45 degree samples welded at 100 and 125 W, the weld shear strength is higher compared to the 60 degree samples. They both can be attributed to the fact that at lower angles, there is little reflection of laser power, resulting in transmission of most of the laser power to the weld interface, and vice-versa for higher angles, as mentioned in section 3.1.1.3.

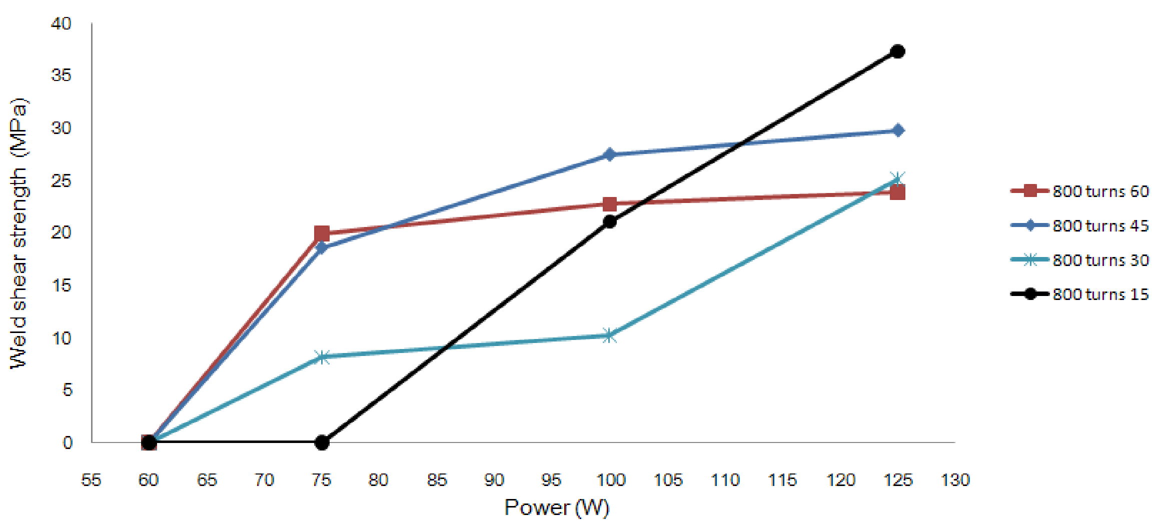

Figure 40: Weld shear strength vs. laser power - 800 laser rotations

A similar trend was seen, when the laser rotations were increased to 1000 (Figure 41). With increasing power, the weld shear strength increased. One of the interesting points to note here is the decrease in shear strength at 125W for both 45˚ and 60˚ samples. This behaviour can be due to two reasons; 1) the samples began to degrade due to excess laser power and 2) increase in weld seam width at higher powers and higher laser rotations. Interestingly, the samples which had major flashes were also the ones which could not withstand higher shear stresses.

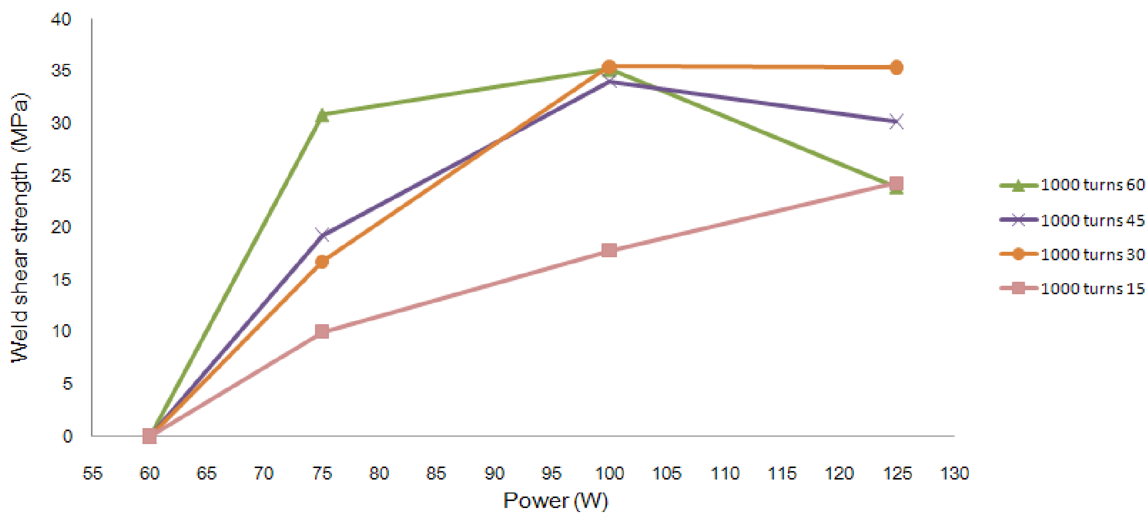

Figure 41: Weld shear strength vs. laser power - 1000 laser rotations

The unwelded nylon-6 bulk material was also tensile stress tested using the MTS tensile tester and the ultimate tensile stress that the material could withstand was observed as 80 MPa. The average weld shear strength of the welded samples was found as 40 MPa. Using these values, the weld factor, which is generally defined as the strength of the weld divided by the tensile stress strength of the unwelded material [3], was calculated as 0.5. The weld factor achieved through the current research work is 50% better than the weld factor of 0.25 achieved in the previous research [1] on laser transmission welding plates and tubes, which produced welds with an average shear strength of 20 MPa.

4.2.3 Local weld quality

When nanoindentation was carried out in the samples, data on the load and depth of sample penetration were recorded continuously. A typical load vs. depth of penetration curve is shown in Figure 42.

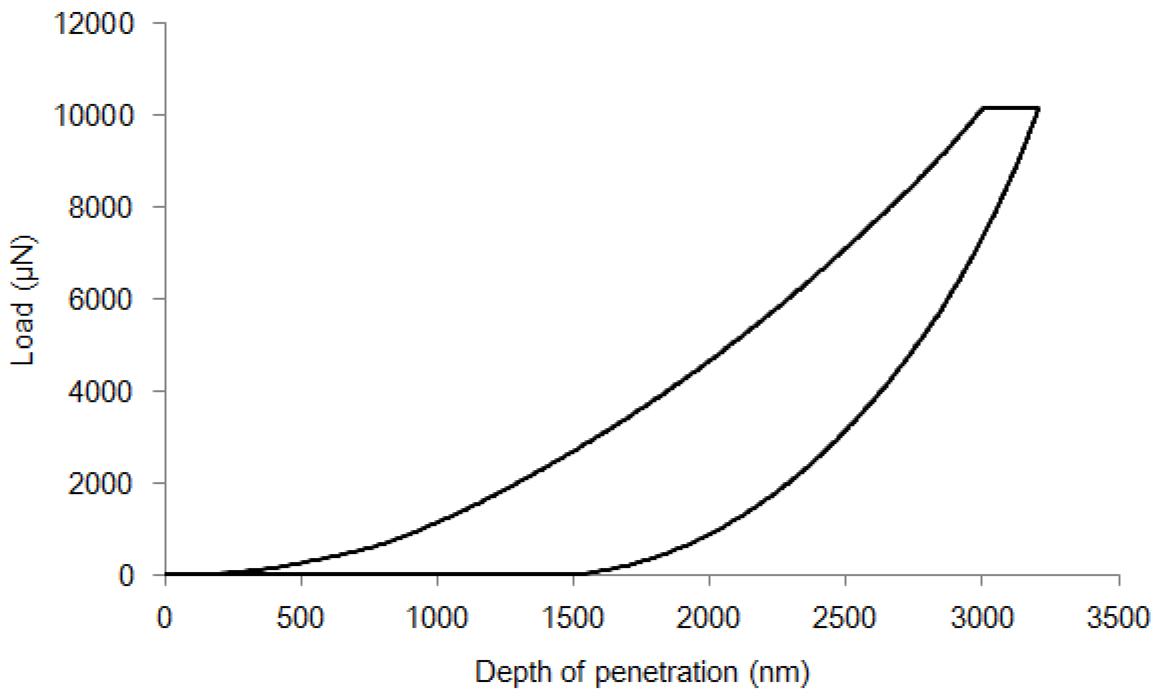

Figure 42: Load-depth of penetration curve from a nanoindent in the weld area of a 60 degree sample welded at 100 W with 1000 laser passes

From each indent, as shown in Figure 34, the modulus was calculated using the procedure outlined in section 4.1.2, to find material property changes at the weld interface. The moduli of indents along the three lines of nanoindentation were plotted over each other as shown in Figure 43, to determine whether the modulus changed when two natural nylon-6 materials are melted and welded together.

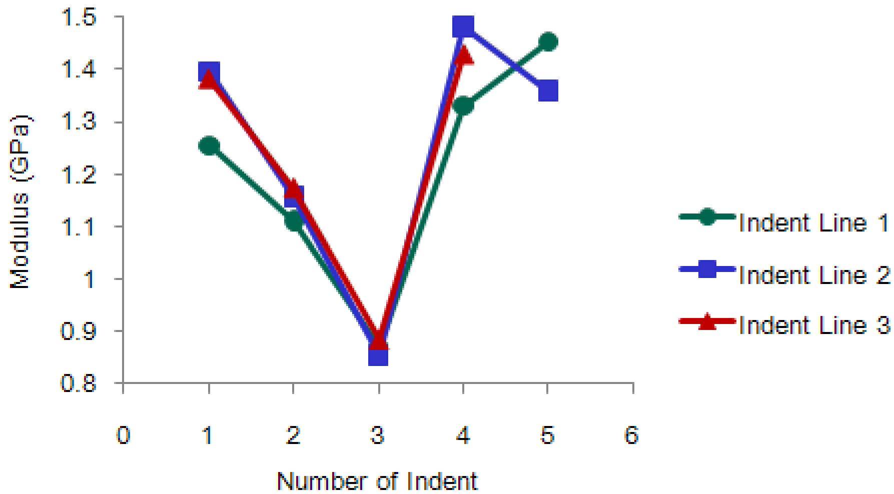

Figure 43: Nanoindentation – Modulus changes at the weld interface

As seen from Figure 43, the modulus decreases at the weld zone, compared to that of the natural unwelded nylon-6 material. The typical value of modulus for natural nylon-6 obtained using nanoindentation was around 1.52 ± 0.05 GPa, which is similar to the values obtained in literature [42]. But for the welded material the modulus decreased to 0.9 ± 0.10 GPa, which is approximately a 35% decrease in modulus from the natural unwelded material. One of the possible reasons for this decrease in modulus is crystallinity, which will be discussed in Chapter 5.

Chapter 5 Crystallinity Characterization

This chapter describes how the crystallinity of the welded nylon-6 material was found using differential scanning calorimetry (DSC) and explains how the crystallinity results obtained differ from the natural nylon-6 material. Explanations for the decrease in modulus at the weld interface due to crystallinity, as mentioned in section 4.2.3 are also elaborated in this chapter.

5.1 Experimental Methodology

DSC testing uses heat flow to calculate the crystallinity of a material, using Equation 2.

$$\text{Crystallinity percentage} = \frac{(\text{Enthalpy of melting}) - (\text{Enthalpy of crystallization})}{(\text{Enthalpy of ultimate crystallinity})} \times 100\ \% \qquad (2)$$

5.1.1 DSC testing

DSC testing was used in this study to compare the crystallinity of the natural nylon-6 and the crystallinity of the welded material. Firstly, samples were scraped using razor blade from the outer skin of the compression molded nylon-6 with 0.2 wt% carbon black plates. Samples were also taken from the core of the plates to see any potential difference in morphology. Then, in order to obtain samples of the welded material, the welded areas of the tensile tested laser absorbent rods were scraped off (approximately 6mg) using a razor blade. These samples were put into hermetic pans. Subsequently, these sealed pans were put in the TA instruments DSC-Q100 machine, which was programmed to heat the samples to 250˚C at a ramp rate of 10˚ C/min.

5.2 Results and Discussion

During the testing process, heat flow data was continuously collected. A typical example of the heat flow curve is shown in Figure 44, and the sample used was taken from the outer skin of the nylon-6 with 0.2 wt % carbon black compression molded plate.

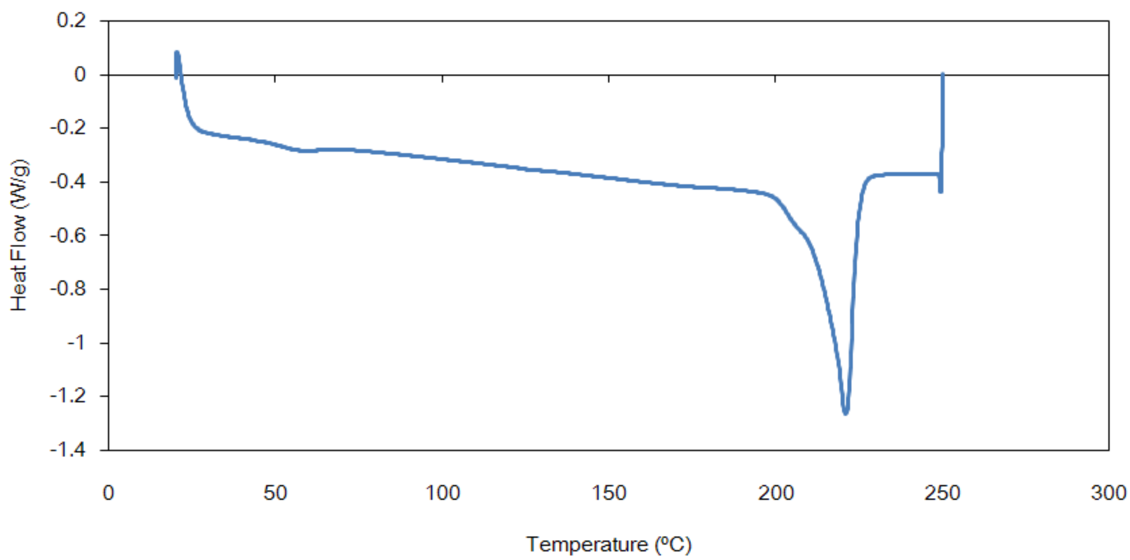

Figure 44: DSC heat flow – Sample from outer skin of compression molded plate

From Figure 44, it can be seen that, the glass transition occurs at 40˚ C and the crystallization curve starts at 55˚ C and finally the melting starts at 200˚C, with its peak at 217˚ C. Also, it is interesting to see that during melting at around 205˚ C, there is a small peak which is characteristic of the γ-form of nylon-6, typically found in the outer skin of a compression molded sample. For all the tested samples, the crystallization curve and the melting curve were isolated using a software to determine the area under the curves as shown in Figure 45 and Figure 46 respectively. These areas represented their respective enthalpies.

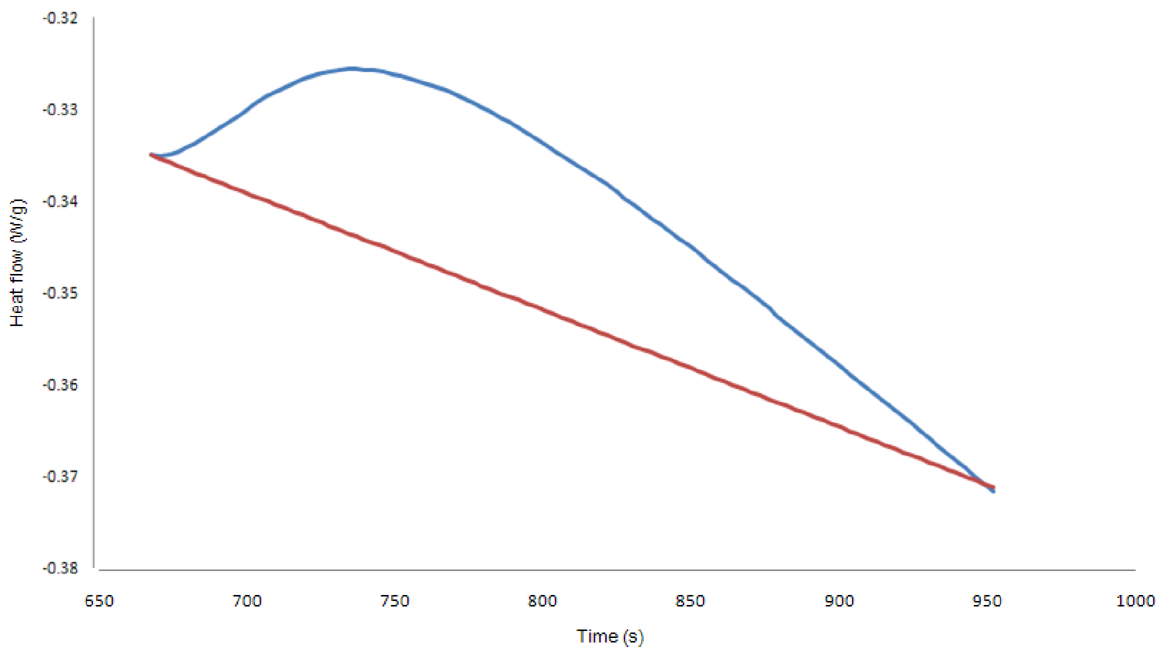

Figure 45: Isolated crystallization peak from the DSC data from the outer skin of the compression molded plate

Using 0.23 J/kg as the enthalpy of ultimate crystallinity [43] of nylon-6, and the enthalpies of melting and crystallization which were calculated from these graphs, the percentage crystallinity of the material was found as 24.42% (using Equation 2).

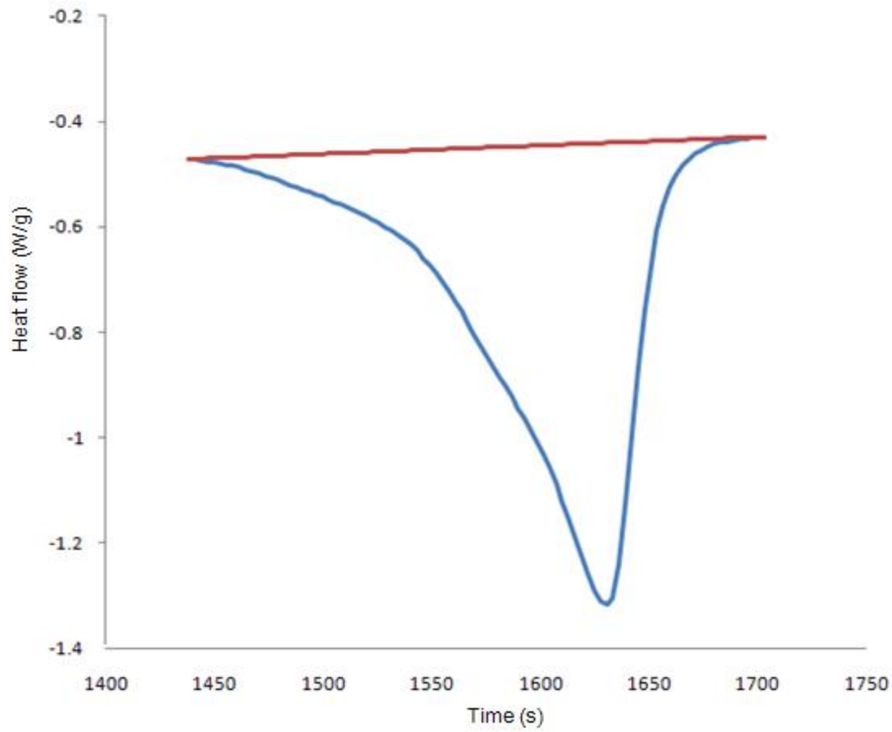

Figure 46: Isolated melting peak from the DSC data from the outer skin of the compression molded plate

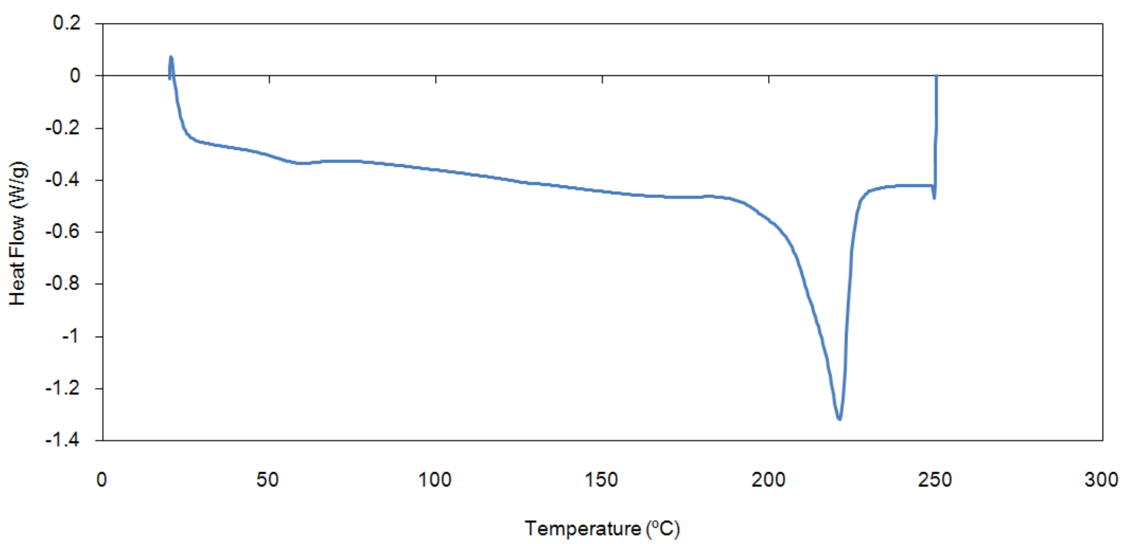

Figure 47: DSC heat flow–Sample from central core of compression molded plate

Using the same compression molded plate, the crystallinity at the core of the sample was tested using DSC and the heat flow graph is shown in Figure 47.

When the sample was taken from the core of the compression molded plate it was clearly seen that the characteristic small peak in the melting region for the γ-form of nylon-6 was missing, which correlates with the literature [29].

The crystallinity percentage of the welded material was calculated in all the welded samples using the same technique.

5.2.1 Change in morphology

When the rods were machined out of the compression molded nylon-6 plates, only the middle portion of the molded plate was exposed. So, all the rods before welding should behave the same way as the graph shown in Figure 47, which has no γ-form of nylon-6. The percentage of γ-form of nylon-6 is important since the modulus of this particular morphology is lower compared to that of the α-form of nylon-6. Thus, any increase in the γ-form after the welding process in the sample can be considered as one of the factors responsible for the lower modulus found by nanoindentation at the weld area. But when the welded materials were tested in DSC, it was found that no new γ crystals of nylon-6 were formed, as there was no characteristic small peak in the melt portion of the heat flow curve, as shown by an example in Figure 48.

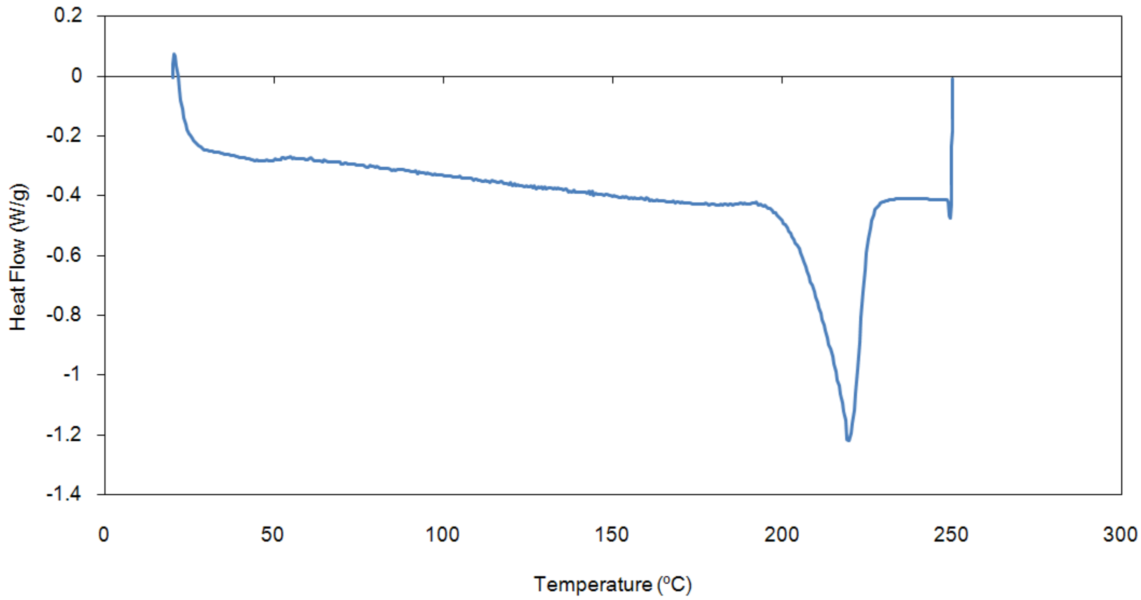

Figure 48: Example of DSC heat flow curve of the welded material from a 30 degree sample welded at 125 W with 1000 laser passes

This proved that the decrease in modulus at the weld zone was not due to the formation of γ-form crystals.

5.2.2 Change in crystallinity percentage

After the crystallinity percentage of the welded material was obtained for different samples, it was compared with the crystallinity percentage of the core of the compression molded nylon-6 with 0.2 wt% carbon black plate. Since the modulus decreases with decrease in crystallinity in semi-crystalline materials such as nylon-6, if there is indeed a decrease in crystallinity at the weld area, then it would explain the decrease in modulus at the weld zone found using nanoindentation.

The crystallinity percentage at the core of the compression molded plate was found as 27.92%. After the welding process, the crystallinity of the welded material samples had dropped to 24.0 ± 1.2%. In order to better understand the change in crystallinity, Figure 49 shows the nanoindented sample cut exactly at the place where the nanoindentation was carried out and the cross-section is viewed from the side.

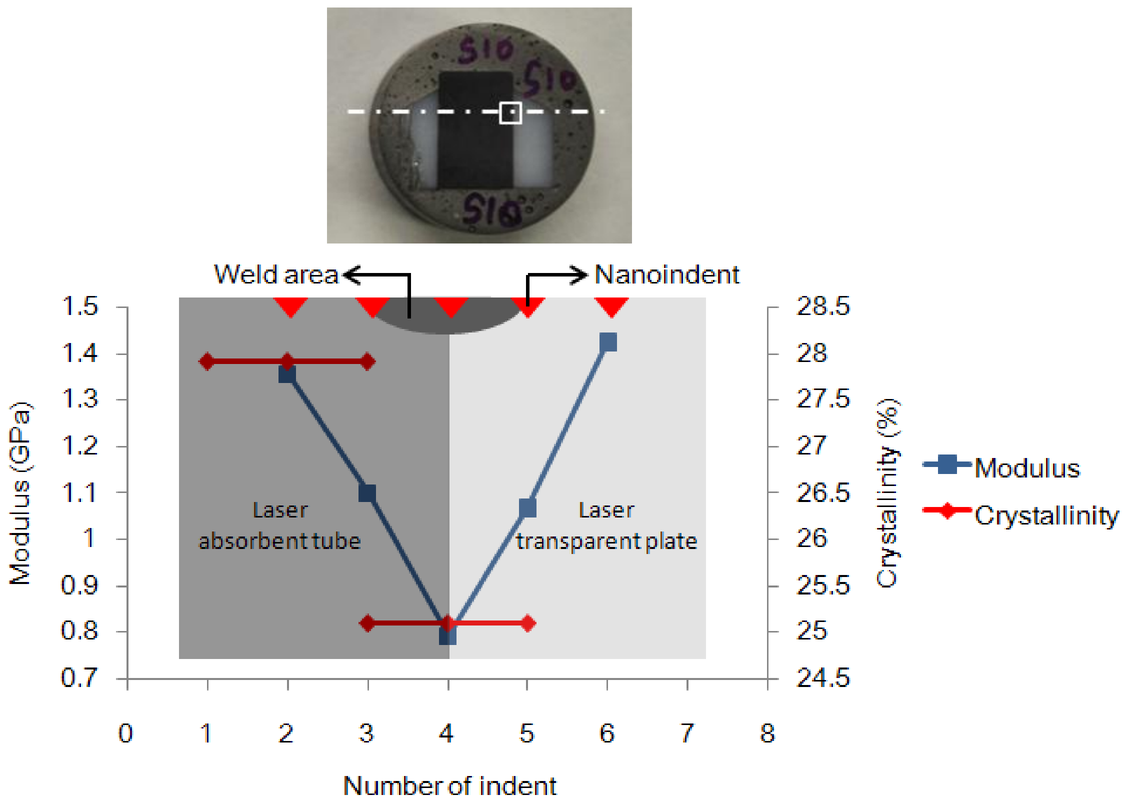

Figure 49: Crystallinity change at the weld area of a 30° sample welded at 125 W with 1000 laser rotations

This conclusively proved that the change in modulus at the weld area is due to the decrease in crystallinity of nylon-6. The reason for this decrease in crystallinity can be due to the fact that during compression molding of the nylon-6 plates, the rate of cooling was being controlled at 15˚ C/min, but the rate of cooling after the welding process was not controlled. Since higher cooling rates produce lesser crystals, the welded material with a higher cooling rate did not have the same time as the compression molded material to organize itself into crystals and hence the decrease in crystallinity.

Chapter 6 Summary, Conclusions and Future Work

This chapter presents the concluding remarks and recommendations for future work. The concluding remarks summarize the results obtained from this research work and emphasize the contributions to the laser transmission welding field. The recommendations suggest the areas that can be developed further in laser refraction welding.

6.1 Summary

This research work investigated the possibility of laser transmission welding of nylon-6 plates and tubes with 0.2 wt% carbon black using laser refraction. A variety of samples with different refraction angles were welded using an extensive test matrix, which used laser parameters such as laser power and number of laser rotations. A visual inspection of the welded samples was carried out and the welded samples were classified as weak, strong, minor flash and major flash welds. At lower laser powers around 60W, either no weld happened or weak welds were obtained. And at very high powers such as 125W, major flash welds happened. And at laser powers of 75W and 100W the preferred strong or minor flash welds were obtained.

Following the completion of welding process, the quality of the welds was tested using a tensile tester. In order to test the strength of this peculiar geometry of welded tubes and plates, a new tensile test fixture was designed and manufactured from steel. Subsequently, the weld seam width of the samples was measured using vernier and transmission light microscopy, so that the tensile stress could be calculated. The results obtained showed that the shear strength of the welds increases with an increase in laser power with 800 and 1000 laser passes, except for the samples welded at 125 W with 1000 laser passes. These samples had a lower shear strength compared to the other samples, as the material started to degrade at the weld interface.

Nanoindentation was then used to find out whether the material property changes at the weld interface, in comparison to the natural nylon-6 material. Results of this local weld quality study showed that the modulus decreased 41% at the weld interface.

Finally, DSC was used to measure the crystallinity levels of the samples before and after welding. The crystallinity percentage after welding was 10% lower compared to the crystallinity levels before welding. Since the crystallinity percentage directly translates to the modulus of a material, the decrease is modulus at the weld area is attributed to this decrease in crystallinity.

6.2 Conclusions

This research conclusively proves that laser refraction welding can be used to weld thermoplastic tubes and plates efficiently. After the samples were welded, they were tested for weld strength. The tests showed that weld quality depends on the refraction angle of the laser transparent plate, the input laser power and the laser power which gets reflected and scattered. In general, the weld strength increases with increasing laser power, until the material starts to degrade due to excess laser power. The material properties of nylon-6 such as modulus change at the weld interface as shown by nanoindentation. The decrease in modulus is due to the decrease in crystallinity at the weld area, as measured through DSC.

6.3 Future work

In this thesis, the concept of welding tubes and plates together using laser refraction welding was demonstrated. But in order to apply this method industrially, the process needs to be optimized thoroughly to produce the strongest and visually appealing weld. To achieve this, a more extensive test matrix needs to be used. This test matrix should investigate power levels in between 75 and 100W, which has been proven by this work to provide strong and minor flash welds. More samples have to be tested for every parameter changed, to reduce the scatter in the data. Also, the strength of the welds with different percentages of carbon black particles needs to be studied in order to possibly achieve stronger welds. The laser contour has to be better controlled to trace the path of laser around the circumference of the tube, as waviness of laser contour was observed in the laser absorbent tube after the welds were tensile tested. And finally more control needs to be exercised on the crystallinity of the laser transparent plates, since the crystallinity of the material affect the laser scattering and the modulus of the welded material.

References

1. Kritskiy, A., *Laser Welding of nylon tubes and plates using conical mirrors*, in *Mechanical and Materials Engineering*2009, Queen's University: Kingston.
2. Woebcken, W., *International Plastics Handbook*1995: Hanser Publications.
3. Harper, C., *Handbook of plastics, elastomers and composites*. 4 ed2002: McGraw-Hill.
4. Grewell, D., Avraham, B., Park, J., *Plastics and composites welding handbook*2003: Hanser.
5. Silverman, E.M., Griese, R.A., *Joining methods for Graphite/PEEK thermoplastic composites.* SAMPE Journal, 1989. **25**(5): p. 34-38.
6. Benatar, A. and T.G. Gutowski, *Ultrasonic welding of PEEK graphite APC 2 composites.* Polymer Engineering & Science, 1989. **29**(23): p. 1705-1721.
7. Ageorges, C., L. Ye, and M. Hou, *Advances in fusion bonding techniques for joining thermoplastic matrix composites: a review.* Composites Part A: Applied Science and Manufacturing, 2001. **32**(6): p. 839-857.
8. Stokes, V., *Vibration welding of thermoplastics. Part I: Phenomenology of the welding process.* Polymer Engineering & Science, 1988. **28**(11): p. 718-727.
9. Sanders, P., *Electromagnetic welding: an advance in thermoplastics assembly.* Materials & Design, 1987. **8**(1): p. 41-45.
10. Stavrov, D. and H. Bersee, *Resistance welding of thermoplastic composites-an overview.* Composites Part A: Applied Science and Manufacturing, 2005. **36**(1): p. 39-54.
11. Hou, M., L. Ye, and Y.W. Mai, *An experimental study of resistance welding of carbon fibre fabric reinforced polyetherimide (CF Fabric/PEI) composite material.* Applied Composite Materials, 1999. **6**(1): p. 35-49.

12. Nakamata, H., *Process for joining different kinds of synthetic resins*, 1987, Google Patents.
13. Becker, F. and H. Potente, *A step towards understanding the heating phase of laser transmission welding in polymers.* Polymer Engineering & Science, 2002. **42**(2): p. 365-374.
14. Kagan, V.A., Bray, R.G., Phino, G.P.,, *Welding with light.* Machine Design, 2000: p. 79-82.
15. I.Kohan, M., *Nylon Plastics*1973: John Wiley and Sons Inc.
16. Grewell, D. and W. Nijenhuis. *TTIR Welding of Aliphatic Polyketone (742)*. 2000.
17. Kagan, V.A., *Innovations in laser welding of thermoplastics: this advanced technology is ready to be commercialized.* 2002.
18. Chen, M., G. Zak, and P. Bates. *Laser absorption coefficient measurement of amorphous polymers for laser transmission welding*. 2006.
19. Chen, M., et al., *Experimental study on gap bridging in contour laser transmission welding of polycarbonate and polyamide.* Polymer Engineering & Science.
20. Kagan, V. and G. Pinho, *Laser transmission welding of semicrystalline thermoplastics-Part II: Analysis of mechanical performance of welded nylon.* Journal of reinforced plastics and composites, 2004. **23**(1): p. 95.
21. Mohan, A., *Modification of Nylon 6 Structure via Nucleation*, in *Fiber and Polymer Science*2009, North Carolina State University: North Carolina. p. 165.
22. Callister, W., *Fundamentals of Materials Science and Engineering*2001: Wiley.
23. Arimoto, H., *Transition of nylon 6.* Journal of Polymer Science Part A: General Papers, 1964. **2**(5): p. 2283-2295.
24. Bradbury, E., et al., *The structure of the gamma form of polycaproamide (Nylon 6).* Polymer, 1965. **6**(9): p. 465-482.

25. Holmes, D., C. Bunn, and D. Smith, *The crystal structure of polycaproamide: Nylon 6.* Journal of Polymer Science, 1955. **17**(84): p. 159-177.
26. Vogelsong, D.C., *Crystal structure studies on the polymorphic forms of nylons 6 and 8 and other even nylons.* Journal of Polymer Science Part A: General Papers, 1963. **1**(3): p. 1055-1068.
27. Aharoni, S., *n-Nylons: Their Syntheis, Structure and Properties.*1997, New York: J. Wiley and Sons.
28. Galeski, A., A.S. Argon, and R.E. Cohen, *Morphology of nylon 6 spherulites in bulk.* Die Makromolekulare Chemie, 1987. **188**(5): p. 1195-1204.
29. Fornes, T. and D. Paul, *Crystallization behavior of nylon 6 nanocomposites.* Polymer, 2003. **44**(14): p. 3945-3961.
30. Shen, L., I.Y. Phang, and T. Liu, *Nanoindentation studies on polymorphism of nylon 6.* Polymer testing, 2006. **25**(2): p. 249-253.
31. Liu, Y., et al., *Crystalline morphology and polymorphic phase transitions in electrospun nylon-6 nanofibers.* Macromolecules, 2007. **40**(17): p. 6283-6290.
32. *New advances in polymer laser welding*. Available from: http://www.dsm.com/nl_NL/downloads/dep/laser_welding_handbook.pdf.
33. Platt, D.K., *Engineering and High Performance Plastics - Market Report*, 2003, Smithers Rapra Technology. p. 35-37,58-60.
34. Platt, D.K., *Engineering and High Performance Plastics - Market Report*, 2003, Smithers Rapra Technology.
35. Platt, D.K., *Engineering and High Performance Plastics - Market Report*, 2003, Smithers Rapra Technology. p. 55-57.
36. Ageorges, C. and L. Ye, *State of the Art in Fusion Bonding of Polymer Composites Fusion Bonding of Polymer Composites*, 2002, Springer London. p. 7-64.

37. Frantz, J., *Joining plastics the sound way.* Machine Design, 1997. **69**(3): p. 61-65.
38. Van de Ven, J.D. and A.G. Erdman, *Bridging gaps in laser transmission welding of thermoplastics.* Journal of Manufacturing Science and Engineering, 2007. **129**: p. 1011.
39. Wilke, L., H. Potente, and J. Schnieders, *Simulation of quasi-simultaneous and simultaneous laser welding.* WELDING IN THE WORLD-LONDON-, 2008. **52**(1/2): p. 56.
40. Lehrle, R., I. Parsons, and M. Rollinson, *Thermal degradation mechanisms of nylon 6 deduced from kinetic studies by pyrolysis-gc.* Polymer degradation and stability, 2000. **67**(1): p. 21-33.
41. Oliver, W. and G. Pharr, *Measurement of hardness and elastic modulus by instrumented indentation: Advances in understanding and refinements to methodology.* J. Mater. Res, 2004. **19**(1): p. 3-20.
42. Bell, G.A., D.M. Bieli ski, and B.D. Beake, *Influence of water on the nanoindentation creep response of nylon 6.* Journal of Applied Polymer Science, 2008. **107**(1): p. 577-582.
43. Perkinelmer. *DSC as problem solving tool: Measurement of percent crystallinity of thermoplastics*. Available from: http://www.perkinelmer.com/Content/applicationnotes/app_thermalcrystallinitythermoplastics.pdf.

Appendix A – Test matrix used in this research

Power (W)	Number of laser rotations	Speed (m/s)	15°	30°	45°	60°	Total
60	800	5.2	1	1	1	1	5
60	1000	5.2	3	3	4	3	17
75	800	5.2	1	1	1	1	4
75	1000	5.2	3	3	4	3	13
100	800	5.2	1	1	1	1	4
100	1000	5.2	3	3	4	3	13
125	800	5.2	1	1	1	1	4
125	1000	5.2	3	3	4	3	13
Total Samples			16	16	20	16	68
Tensile testing, optical microscopy, DSC			12	12	16	12	52
Reflection and transmission microscopy, SEM, nanoindenter			4	4	4	4	16

Appendix B – Tensile test data

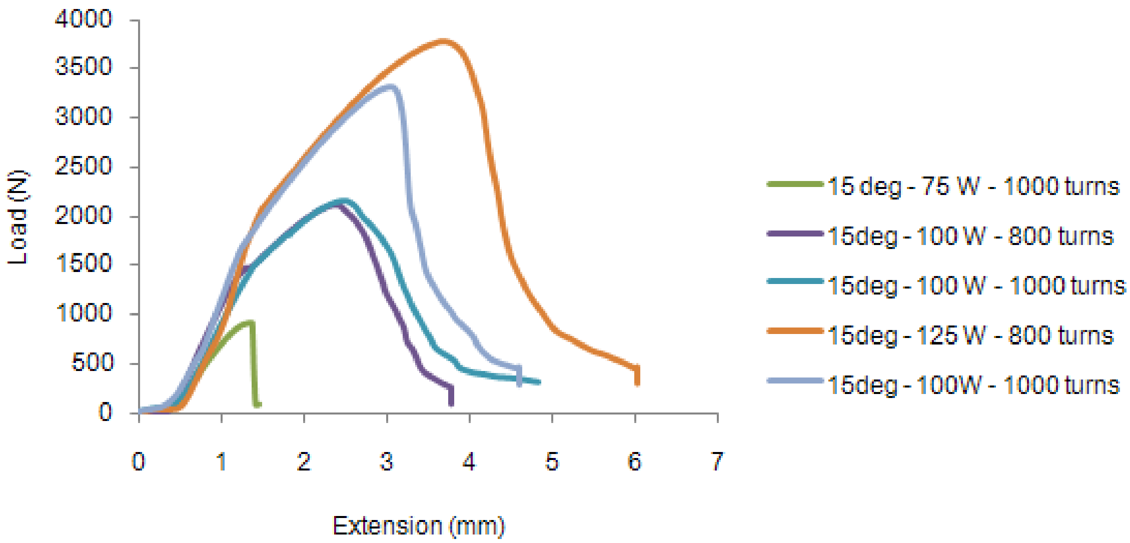

Figure 50: Load-extension curves of 15 degree samples

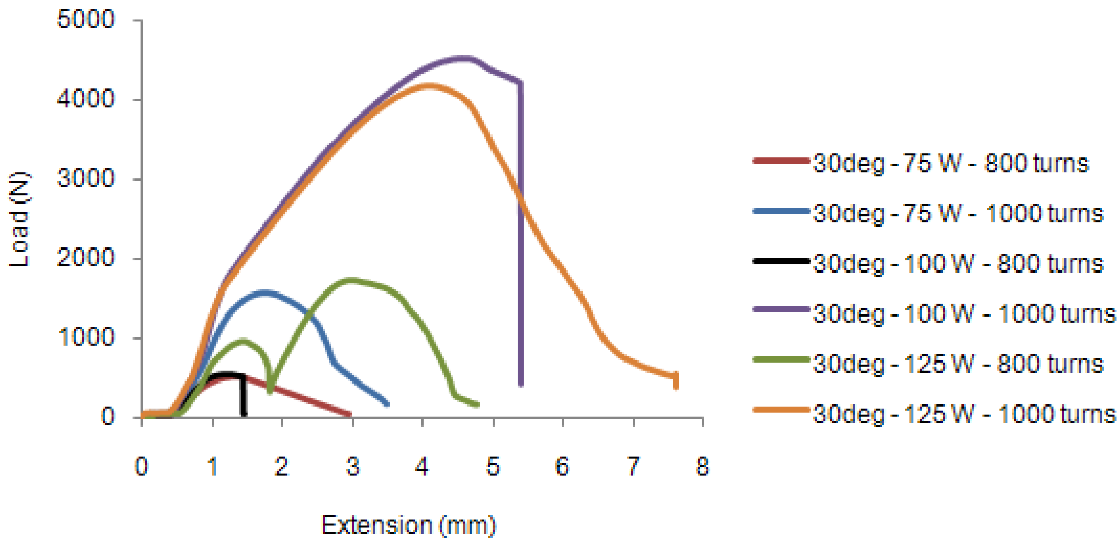

Figure 51: Load-extension curves of 30 degree samples

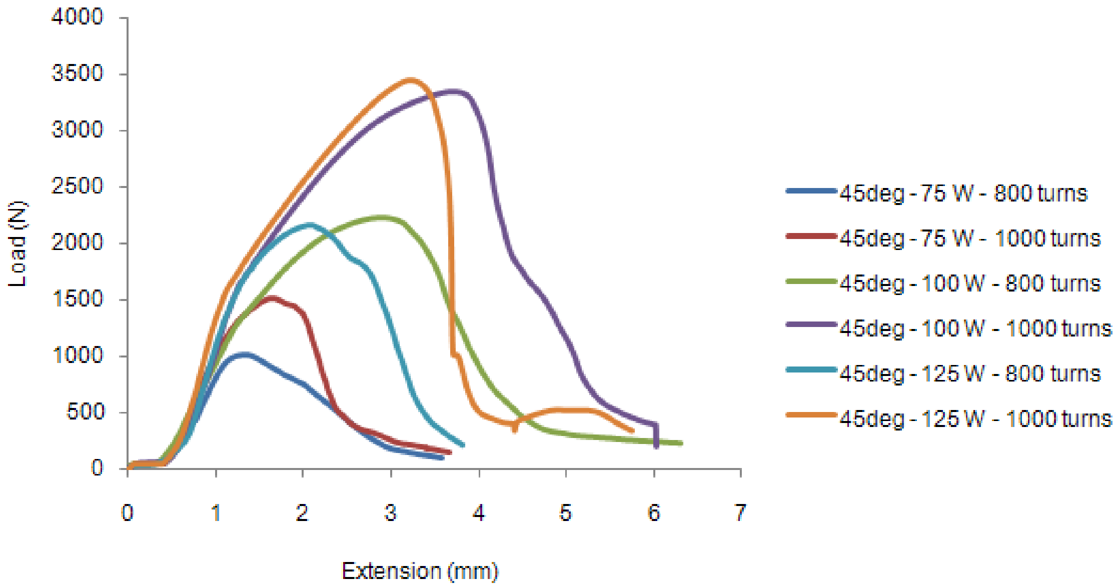

Figure 52: Load-extension curves of 45 degree samples

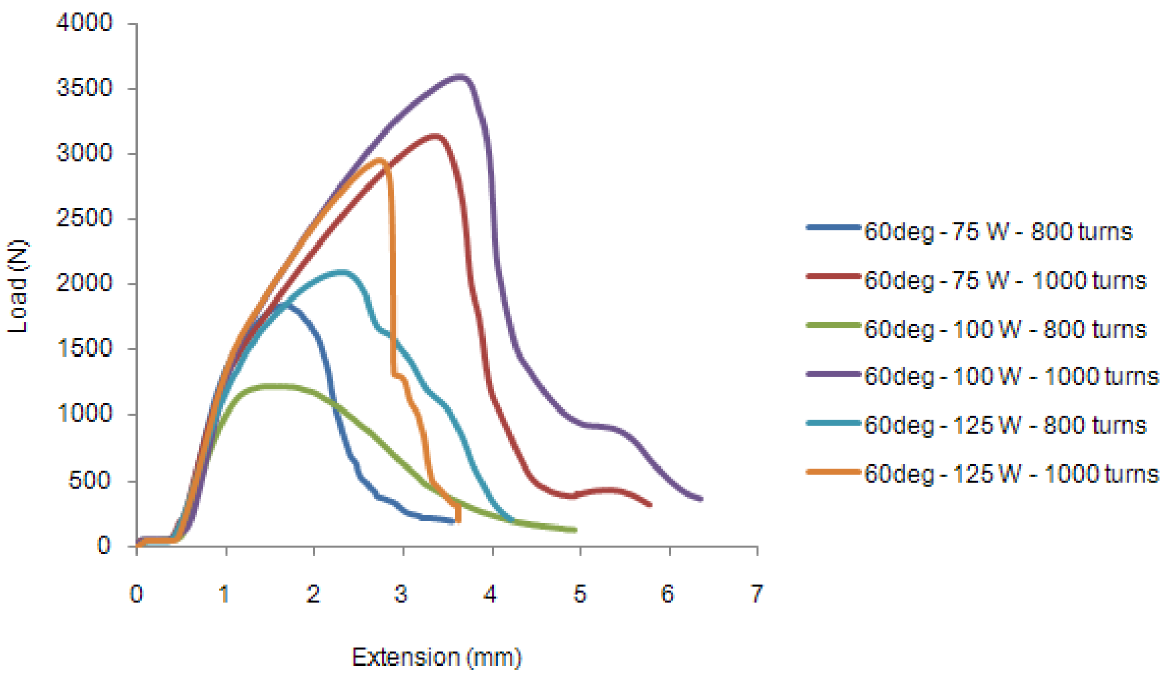

Figure 53: Load-extension curves of 60 degree samples

Appendix C – Nanoindentation data

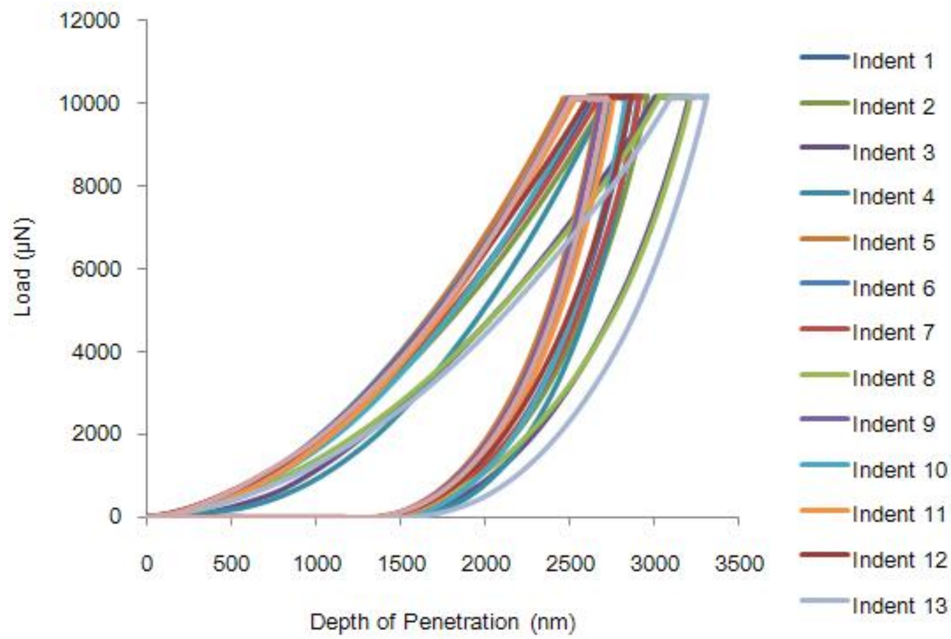

Figure 54: Load-Depth of penetration nanoindentation curves of a 15 degree sample welded at 125 W with 1000 turns

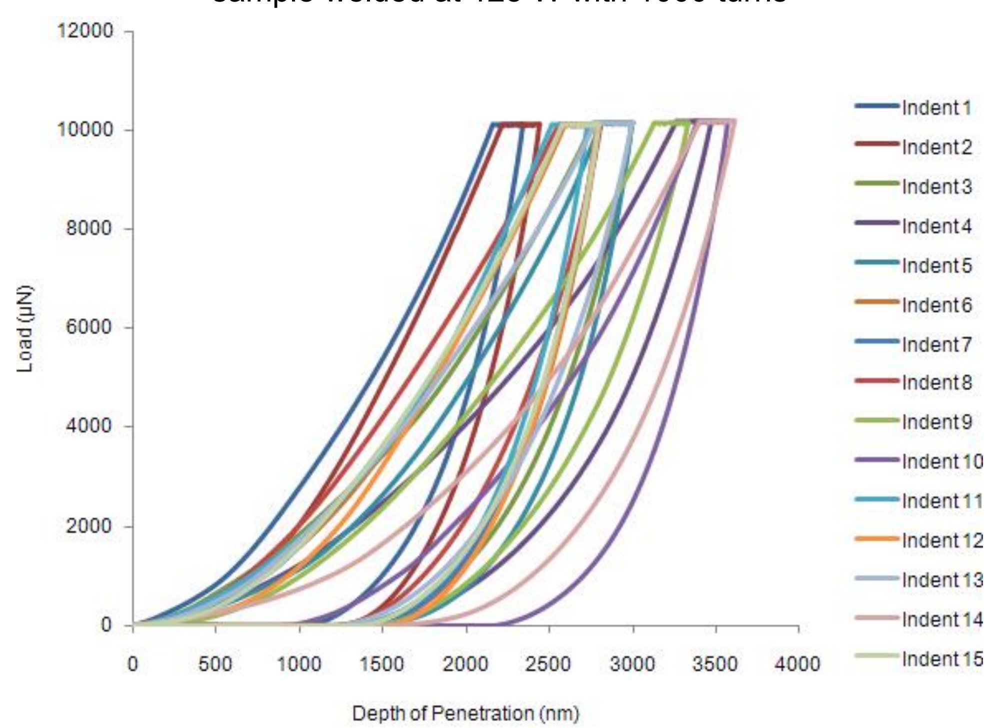

Figure 55: Load-Depth of penetration nanoindentation curves of a 30 degree sample welded at 125 W with 1000 turns

Appendix D – DSC data

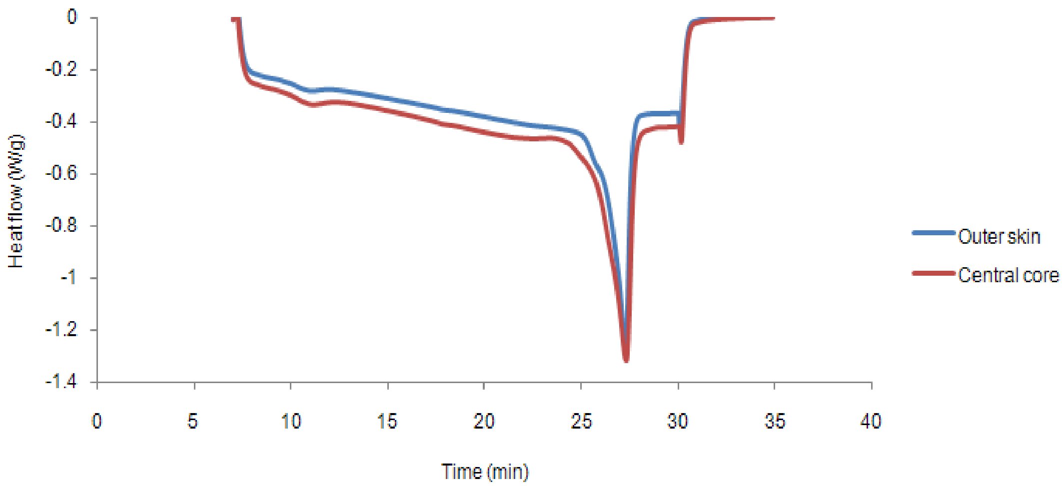

Figure 56: Heat flow curves of samples taken from the outerskin and the central core of the compression molded plates

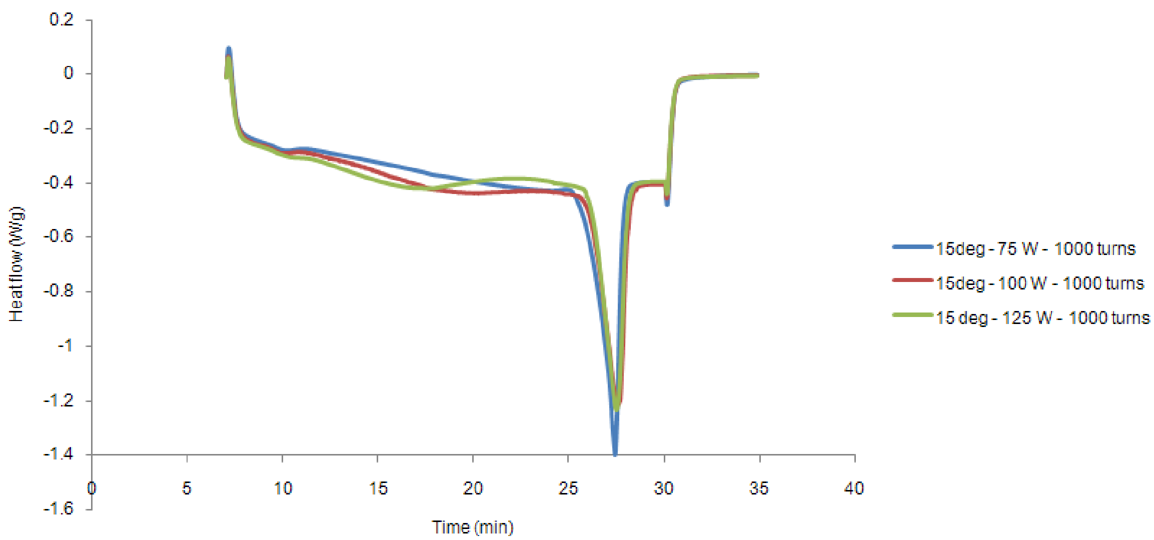

Figure 57: Heat flow curves of 15 degree samples welded at different laser power with 1000 rotations

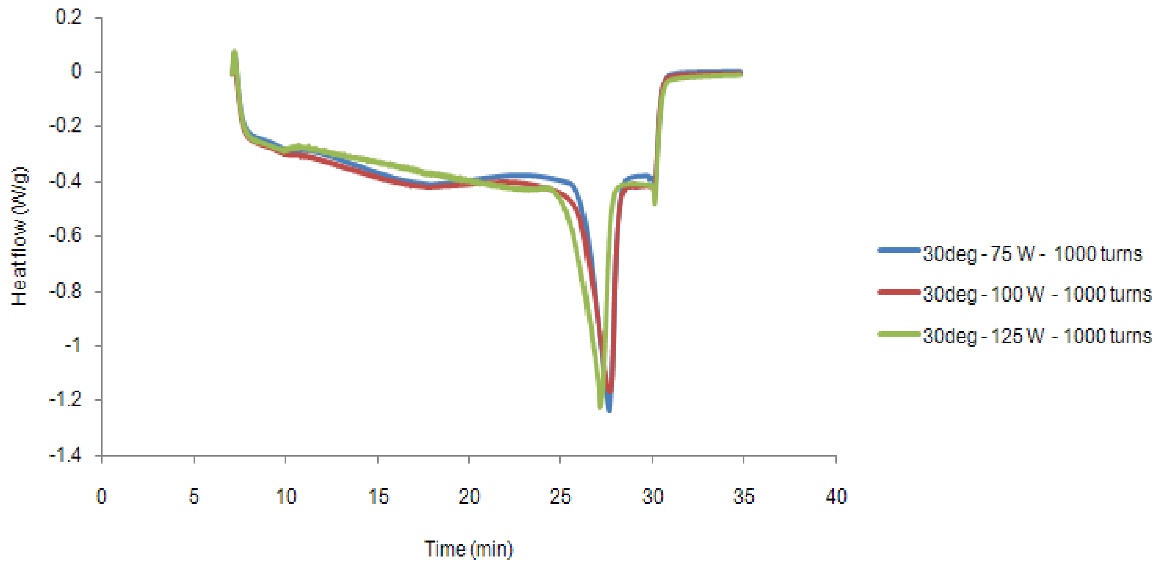

Figure 58: Heat flow curves of 30 degree samples welded at different laser power with 1000 rotations

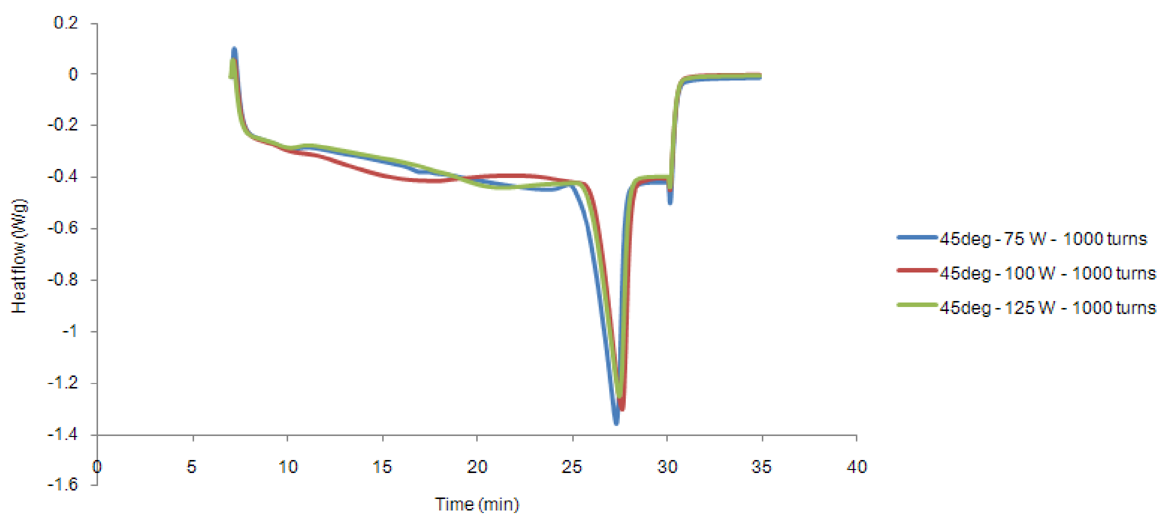

Figure 59: Heat flow curves of 45 degree samples welded at different laser power with 1000 rotations

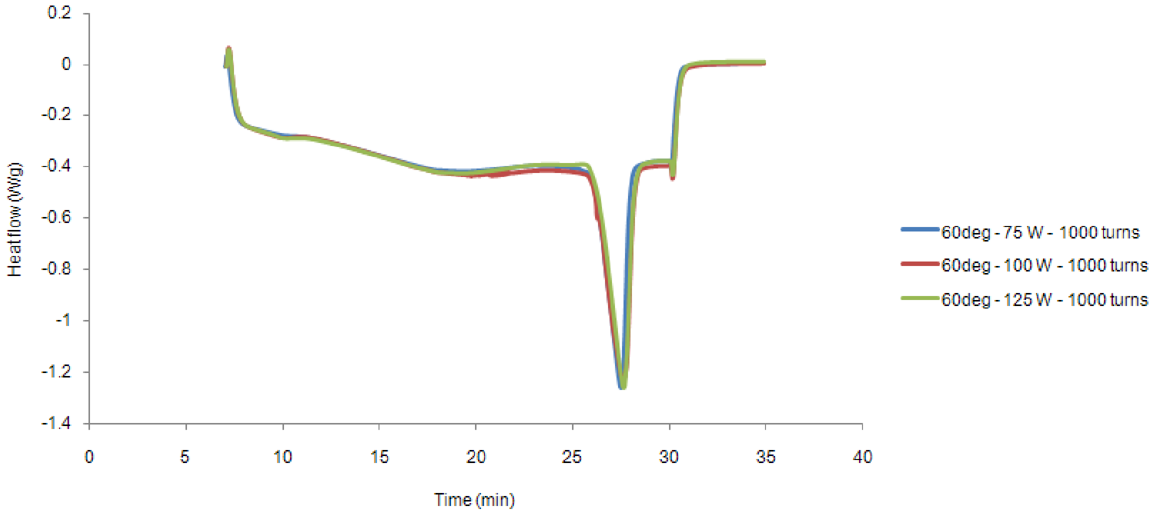

Figure 60: Heat flow curves of 60 degree samples welded at different laser power with 1000 rotations